Geosciences **2013**, *3*, 176-215; doi:10.3390/geosciences3020176

OPEN ACCESS

geosciences

ISSN 2076-3263

www.mdpi.com/journal/geosciences

Article

Structural Evolution of the East Sierra Valley System (Owens Valley and Vicinity), California: A Geologic and Geophysical Synthesis

Calvin H. Stevens [1,*], Paul Stone [2] and Richard J. Blakely [2]

[1] Department of Geology, San Jose State University, 1 Washington Square, San Jose, CA 95192, USA

[2] U.S. Geological Survey, 345 Middlefield Road, Menlo Park, CA 94025, USA;
E-Mails: pastone@usgs.gov (P.S.); blakely@usgs.gov (R.J.B.)

* Author to whom correspondence should be addressed; E-Mail: calvin.stevens@sjsu.edu;
Tel.: +1-408-924-5029; Fax: +1-408-924-5053.

Received: 1 February 2013; in revised form: 30 March 2013 / Accepted: 30 March 2013 / Published: 22 April 2013

Abstract: The tectonically active East Sierra Valley System (ESVS), which comprises the westernmost part of the Walker Lane-Eastern California Shear Zone, marks the boundary between the highly extended Basin and Range Province and the largely coherent Sierra Nevada-Great Valley microplate (SN-GVm), which is moving relatively NW. The recent history of the ESVS is characterized by oblique extension partitioned between NNW-striking normal and strike-slip faults oriented at an angle to the more northwesterly relative motion of the SN-GVm. Spatially variable extension and right-lateral shear have resulted in a longitudinally segmented valley system composed of diverse geomorphic and structural elements, including a discontinuous series of deep basins detected through analysis of isostatic gravity anomalies. Extension in the ESVS probably began in the middle Miocene in response to initial westward movement of the SN-GVm relative to the Colorado Plateau. At *ca.* 3–3.5 Ma, the SN-GVm became structurally separated from blocks directly to the east, resulting in significant basin-forming deformation in the ESVS. We propose a structural model that links high-angle normal faulting in the ESVS with coeval low-angle detachment faulting in adjacent areas to the east.

Keywords: Sierra Nevada; White-Inyo Mountains; Coso Range; Indian Wells Valley; Basin and Range; Walker Lane; Eastern California Shear Zone; Panamint Detachment

---

1. Introduction

The Sierra Nevada-Great Valley microplate (SN-GVm) has been moving westward and more recently northwestward with respect to the North American craton and the Colorado Plateau since the middle Cenozoic, e.g., [1–5], leaving an extended terrane in its wake (Figure 1). This displacement has resulted in the development of extensional basins and dextral slip on numerous faults in eastern California and western Nevada, a region commonly referred to as the Walker Lane-Eastern California Shear Zone (WL-ECSZ), which accounts for about 20% of the dextral movement between the Pacific and North American plates, e.g., [6].

A particularly interesting and structurally significant part of the WL-ECSZ is the linear valley system ("East Sierra Valley System" of this report) that has developed along the eastern margin of the southern and central parts of the SN-GVm (Figure 1). The principal component of this system (Figure 2) is the 125-km-long Owens Valley, but it also includes Rose and Indian Wells valleys to the south and Chalfant, Round, and Long valleys to the north. The East Sierra Valley System (ESVS), which delineates the western margin of the Basin and Range Province, is especially important tectonically because this is where the SN-GVm is actively dissociating from the North America craton. In addition, the north-northwest-trending ESVS (Figure 2), which strikes at a significant angle to the present northwestward motion of the SN-GVm away from the North American craton, is the locus of much of the present right-lateral displacement and extension in the Basin and Range Province [7]. Modern activity in the region was demonstrated by the 1872 Owens Valley earthquake, during which as much as 10 m of right-lateral slip occurred [8], and by the 1986 Chalfant Valley earthquake during which about 1 m of right-lateral slip took place [9].

The geology and structural evolution of the ESVS region have been the subject of many recent investigations, a large number of which have focused on late Cenozoic faulting and related deformation, e.g., [3,8,10–14]. Numerous additional studies have investigated a variety of other topics including pre-late Cenozoic structural evolution, e.g., [15,16], geomorphology [17,18], active deformation based on geodetic and GPS data, e.g., [19–21], thermochronometry, e.g., [22–24], subsurface structure based on reflection seismic and lithologic log data, e.g., [25], seismicity, e.g., [13,26], and hydrology, e.g., [27]. Because much of the research has focused on specific areas, topics, or intervals of geologic time, and because the resulting literature is so voluminous, gaining an overview of the geologic history and evolution of the entire ESVS region is difficult, although Phillips [28] recently provided a valuable summary of late Miocene and younger events with emphasis on the history of the paleo-Owens River drainage.

This paper has a dual purpose: (1) to summarize geological data developed for this area, and (2) to develop a model to explain the major geologic features. Therefore we comprehensively reviewed and analyzed the available literature in an attempt to synthesize the results of numerous diverse investigations into a coherent interpretation of the history and mechanisms involved in the development of the entire ESVS region. We enhanced this synthesis through the use of isostatic gravity data, which provide a very useful tool for elucidating the subsurface configuration and depth of sedimentary basins. As part of our synthesis, we recognize for the first time three structural zones that form boundaries between different segments of the valley system, emphasize the importance and independent development of the different structural blocks that make up the ESVS, and present a tectonic model that links the

mostly high-angle faulting that characterizes the ESVS proper with coeval low-angle detachment faulting that typifies the region directly to the east. We also show that the ESVS evolved in several stages beginning with initiation of strike-slip faulting between Late Cretaceous and early Miocene time, followed by extensional deformation beginning in the middle Miocene, and concluding with transtensional deformation that continues today. Finally, we briefly discuss the possibility that the ESVS might be evolving into a rift system like the Gulf of California [29,30], with which it bears intriguing tectonic similarities. Although some of our interpretations are speculative, we present this synthesis with the intention of stimulating future research that might produce more definitive results.

In addition to the types of recent investigations noted above, much research also has been concerned with the deep lithospheric processes inferred to have driven the structural and tectonic evolution of the Sierra Nevada and ESVS region, e.g., [5,31–33]. While the importance of this research is obvious, further discussion of the deep lithosphere is largely beyond the scope of this study, which instead focuses primarily on the structural evolution of upper crustal features extending from the earth's surface to depths of about 10 km.

Figure 1. Map showing location of East Sierra Valley System and inferred net displacement of the Sierra Nevada relative to the Colorado Plateau as a result of extensional deformation beginning at *ca.* 16 Ma [1,2]. Relative motion of the Sierra Nevada was westerly until *ca.* 10 Ma and then changed to northwesterly.

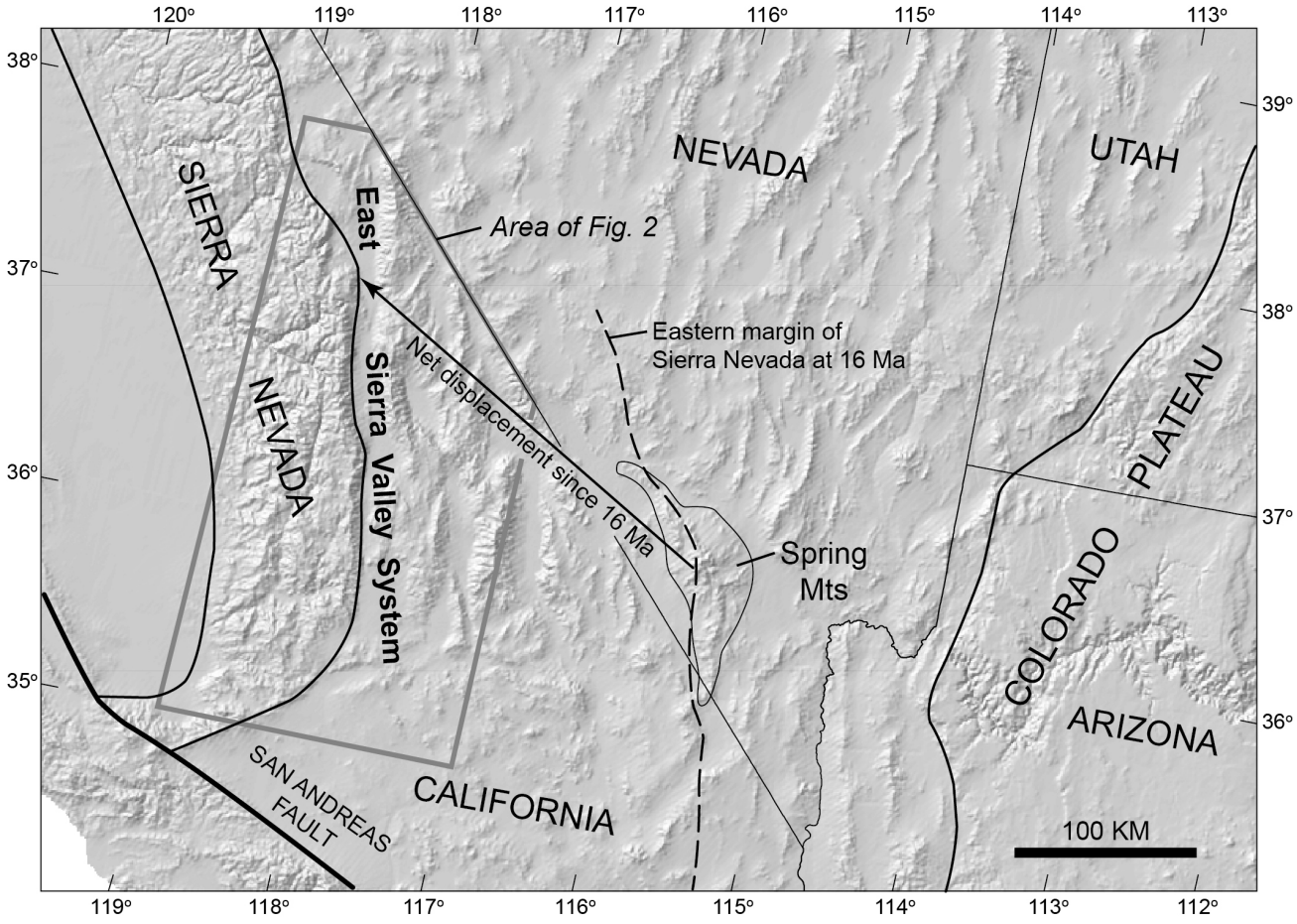

Figure 2. Map showing major geomorphic and cultural features along the western margin of the Basin and Range Province east of the central and southern margins of the Sierra Nevada. AH = Alabama Hills; B = Bishop; BP = Big Pine; CF = Coyote Flat; CW = Coso Wash; DH = Darwin Hills; DM = Dry Mountain; DP = Darwin Plateau; DW = Darwin Wash; FLV = Fish Lake Valley; Ind = Independence; LP = Lone Pine; MC = Mazourka Canyon; ML = Mono Lake; MM = Mount Morrison; PF = Papoose Flat; PH = Poverty Hills; SRF = Santa Rita Flat Pluton; SRH = Santa Rosa Hills; TR = Tinemaha Reservoir; WE = Waucoba Embayment. Cross section X-X' is shown in Figure 13.

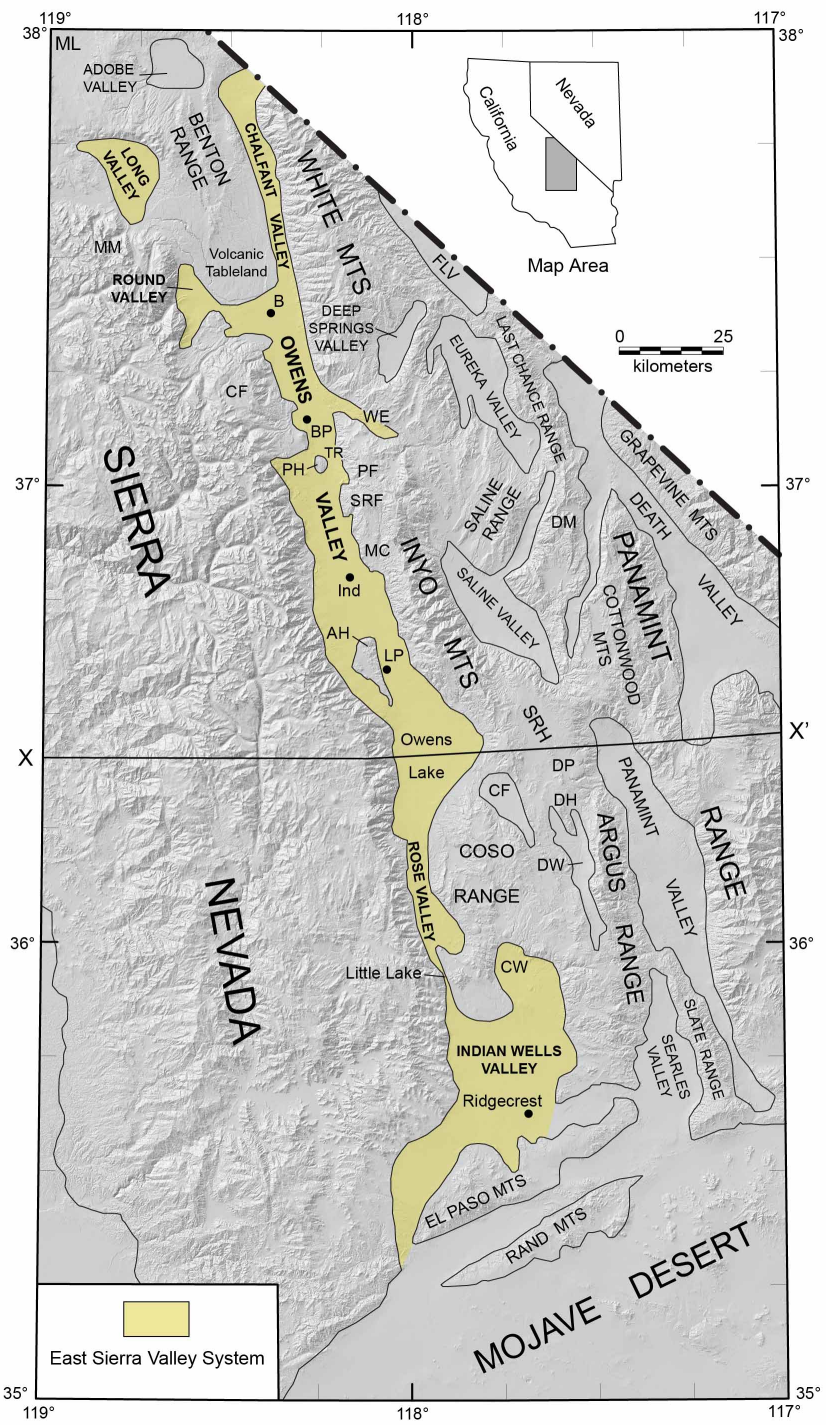

2. Geologic and Geophysical Framework

The valleys that form the ESVS (Figure 2) are bounded on the east and west by mountain ranges primarily composed of Neoproterozoic to Mesozoic sedimentary rocks, Mesozoic volcanic rocks, and Late Cretaceous and older batholithic plutonic rocks. Although the ESVS is tectonically active, post-batholithic deformation in the region, including exhumation and tilting of the Inyo Mountains and possible dextral faulting in the ESVS, extends back to the Late Cretaceous or Early Cenozoic, e.g., [15,16,24,34,35], with extension leading to development of the modern valley system beginning in the middle Miocene, e.g., [17,22,24,36].

The structural and geomorphic features represented in the modern valley system are largely due to faults developed as a consequence of recent uplift and lateral displacement of the SN-GVm. Within the ESVS, Quaternary faulting is ubiquitous (Figure 3). By contrast, the high mountains bordering the ESVS, the Sierra Nevada on the west and the White-Inyo and Argus ranges on the east, show only local evidence of Quaternary faulting except in the southern Sierra Nevada, where recent studies have shown significant faulting to have been active as recently as about 18 ka [37–39]. Regardless, those mountain blocks are here treated as relatively rigid blocks that bound a valley system where most of the active deformation is concentrated.

Both extensional faults and dextral strike-slip faults occur within and border the ESVS. On the west side of the ESVS, down-to-east normal range-front faults extend essentially continuously from Indian Wells Valley northward to Long Valley, e.g., [12] (Figures 2 and 3), although between the Poverty Hills and Round Valley much of the displacement has taken place by downwarping [13,40]. On the east side of the ESVS, the western margins of the White Mountains, Inyo Mountains, and Argus Range are marked by down-to-west normal and/or oblique-slip faults, parts of which lack evidence of late Quaternary displacement.

Dextral strike-slip displacement and extension are presently occurring throughout the length of the ESVS. Numerous geologic and geodetic studies have produced estimates of late Pleistocene to Holocene rates of horizontal extension and right-lateral movement across the ESVS, with particular emphasis on the Sierra Nevada Frontal Fault and the Owens Valley Fault south of latitude 37° N, e.g., [7,8,11,19,41–43]. These studies suggest rates of horizontal extension and right-lateral displacement on the order of 0.5–1 mm/year and 2–3 mm/year, respectively, equating to about 1.5–3 km of extension and 6–9 km of right-lateral movement in the last 3 million years.

In the south, dextral strike-slip displacement is presently occuring along the Owens Valley Fault, which cuts obliquely across the axis of the valley, e.g., [8] (Figures 2 and 3). South of Owens Valley, right slip has been documented on both the Little Lake Fault [44,45] and the Airport Lake Fault in Indian Wells Valley [44,46] (Figure 3). To the north in the general area of Big Pine, strike-slip displacement on the Owens Valley Fault is transferred eastward to the en echelon White Mountains Fault and ultimately farther eastward across the White-Inyo Range to the Fish Lake Valley Fault, e.g., [47–49] (Figure 3). Right-lateral movement on the White Mountains fault is reduced by about 1 mm/year from that on the Owens Valley Fault due to the transfer of slip to the east [7].

Figure 3. Map showing Quaternary faults in east-central California [39,50]. Abbreviated fault names are as follows: ALFZ = Airport Lake Fault Zone; BF = Breckenridge Fault; CWF = Coso Wash Fault; LLF = Little Lake Fault; PH = Poverty Hills; WHMFZ = Wild Horse Mesa Fault Zone [51].

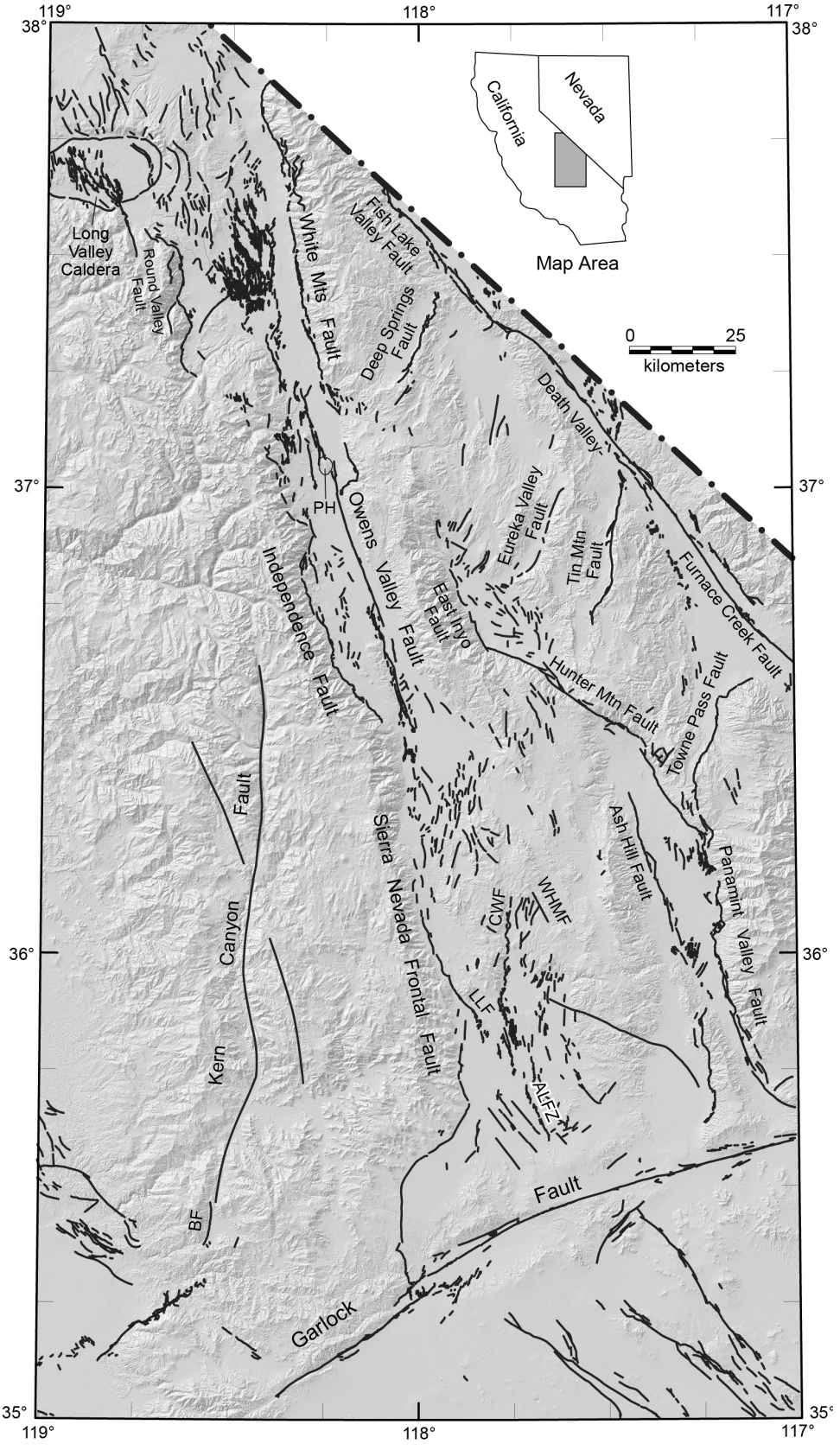

Recent studies, e.g., [15,16,34] have reported evidence of *ca.* 65 km of total right-lateral displacement across the ESVS during at least two episodes of movement since Late Cretaceous time. Regional relations summarized by Bartley *et al.* [16] suggest that less than 10 km of this displacement has taken place since the early or middle Miocene, the remaining 55 km or more having taken place earlier. Evidence presented later indicates that the present transtensional regime with significant right-lateral faulting probably did not begin in the ESVS until the late Pliocene *ca.* 2.8 Ma [24] or 3 Ma [22].

Isostatic gravity data are especially useful for interpreting vertical fault displacements, basin shapes, and sediment thicknesses, e.g., [52]. In the Basin and Range Province, gravity data reflect to first order the contrast between high-density rocks that underlie the ranges and low-density deposits that fill the basins. The deeper parts of the sediment-filled valleys are marked by large negative gravity anomalies that reflect the amount of vertical displacement on adjacent faults. In the ESVS (Figure 4), large negative gravity anomalies extend discontinuously from north of the El Paso Mountains through Rose Valley and Owens Valley to the Bishop area, where the valley system bifurcates, one arm extending northward into Chalfant Valley and the other northwestward into Round Valley [27,40,53–55]. Mathematical inversion of the isostatic gravity anomalies allows an estimate of subsurface sediment thicknesses (*i.e.*, depth to basement) beneath the valleys [56,57] (Figure 5). The inverse method iteratively separates observed gravity into two components: the gravity field of basement rocks and the gravity field caused by low-density basin fill. Then estimates of basin-fill thickness are made from the latter component [57].

A striking feature of the ESVS is the discontinuous nature of the deep basins that extend northward from Indian Wells Valley through Owens Valley to Chalfant and Long valleys (Figure 5). All of these basins are bounded by known or inferred faults on which significant normal displacement has occurred, including faults which may be predominantly dextral (the Owens Valley-White Mountains fault system).

In Owens and Chalfant valleys, the eastern margin of this deep basin system is sharply marked by the West Inyo and White Mountains faults except at an apparent divide between the Owens and Bishop basins near latitude 37° N, where Cenozoic deposits are very thin (Figures 4 and 5). South of Owens Lake the deep basin system is constricted by the Coso Range (Figure 2). Farther south in Indian Wells Valley, the eastern margin of the deep basins is marked by the Little Lake and Airport Lake faults (Figure 5). Here we tentatively follow Pluhar *et al.* [58] in connecting the West Inyo and West Argus faults, although no major sedimentary basin has formed along this part of the fault. However, the Wild Horse Mesa Fault, a northwest-trending seismic source zone, occurs along this trend, e.g., [51], and recent seismic activity has taken place along the same trend to the north in southeastern Owens Lake [59].

The western margin of the deep basin system coincides with the Owens Valley Fault east of the Alabama Hills, whereas to the south in Indian Wells Valley, the western boundary lies close to the Sierran front. To the north the western boundary lies east of the Coyote Warp, a sloping bedrock surface that defines the eastern margin of the Sierra Nevada in this area, and farther north it lies west of Round and Long valleys along the Sierran front [53] (Figure 5).

Figure 4. Isostatic gravity map of east-central California [53]. Shading of the gravity highs and lows simulates a shaded relief map of topography with lighting from the northeast. For abbreviations see caption for Figure 2.

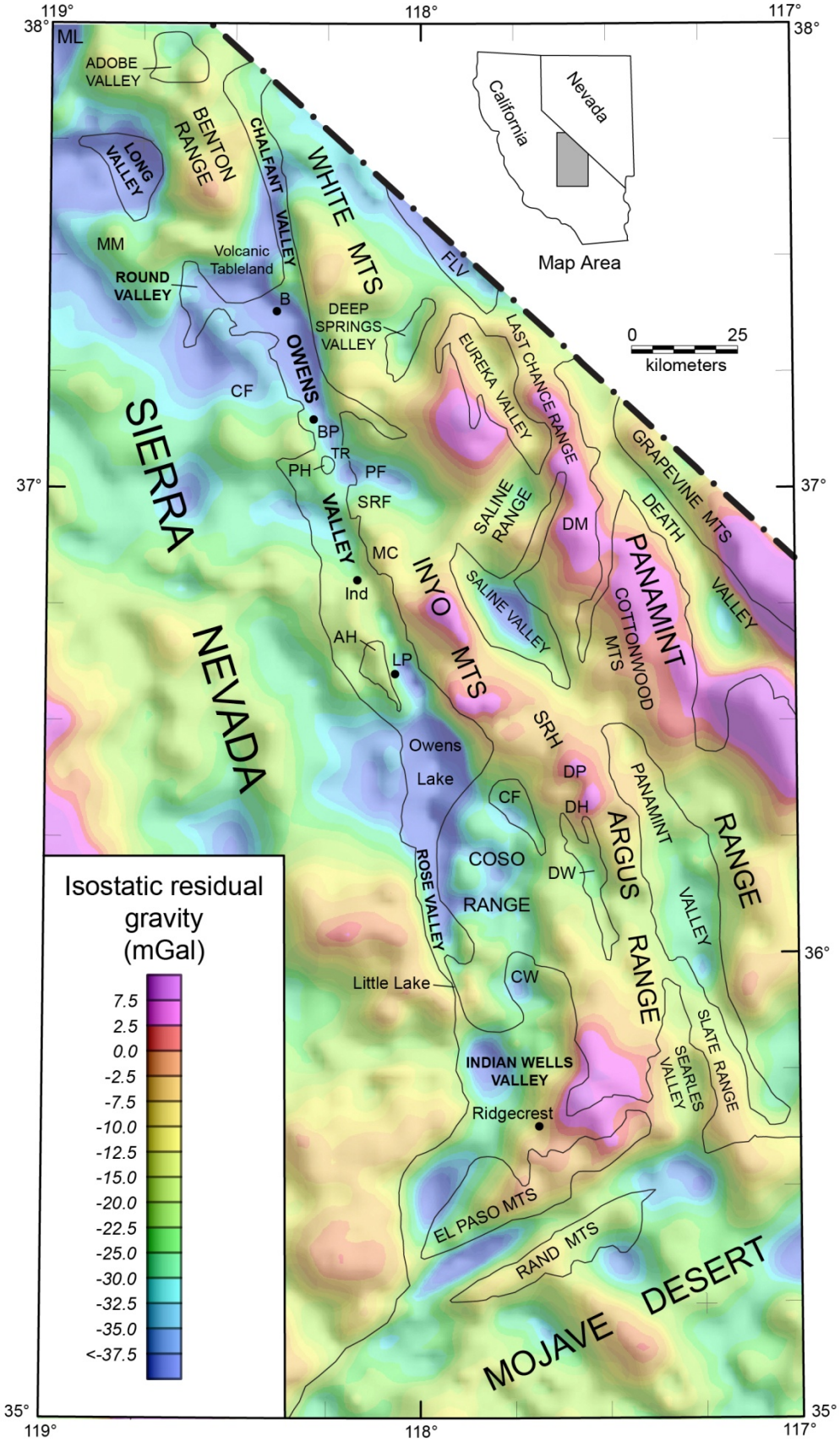

Figure 5. Map showing interpreted thickness of Cenozoic deposits and major faults outlining the deep basins, based on inversion of gravity data [56]. Connection between West Inyo and Southwest Argus faults from Pluhar *et al.* [58]. ALFZ = Airport Lake Fault Zone; CWF = Coso Wash Fault; EIF = East Inyo Fault; LLF = Little Lake Fault. A-A' to H-H' indicate lines of cross sections and gravity profiles shown in Figure 10.

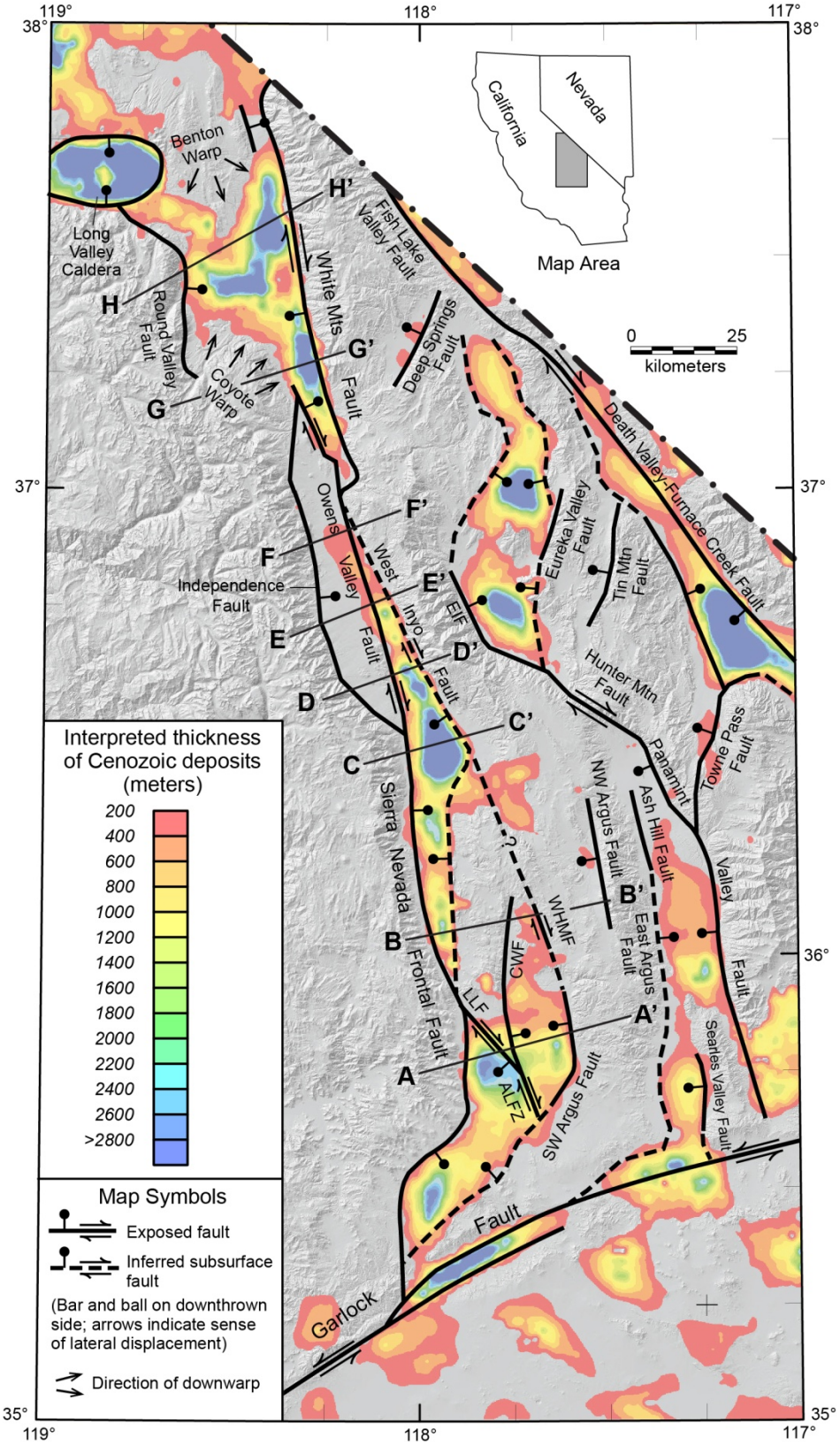

The Poverty Hills, a small, isolated bedrock block composed of upper Paleozoic sedimentary rocks and Mesozoic plutonic rocks [60,61], lies just south of a 3-km left step in the Owens Valley Fault in the central part of Owens Valley (Figure 6). Different workers have interpreted these hills as (1) a transpressional basement uplift caused by this restraining bend in the dextral fault zone [12,62,63]; (2) a fault block displaced from the Inyo Mountains to the east [23], possibly from a prominent bight in the western flank of that range 6 km to the ESE (Figure 6) [64]; and (3) a large Quaternary slide block derived either from the Sierra Nevada to the west [40] or from the Inyo Mountains to the east [49]. We favor the slide block interpretation, which is consistent with the location of the Poverty Hills directly above a steep gravity gradient that defines the western margin of the Bishop Basin (Figure 6). The most likely source of the slide block is in the Inyo Mountains, where rocks of similar age and lithology as those in the Poverty Hills are exposed [49], in contrast to the Sierra Nevada directly to the west where such rocks are absent [54]. It is possible that the slide block has been uplifted by transpressional deformation at the restraining bend in the Owens Valley Fault since its initial emplacement.

Figure 6. Map showing Quaternary faults in central Owens Valley and isostatic residual gravity contours in vicinity of the Poverty Hills [50,53]. Note left step in trace of Owens Valley Fault north of Poverty Hills and steep gravity gradient coincident with Poverty Hills. B = bight in northern Inyo Mountains.

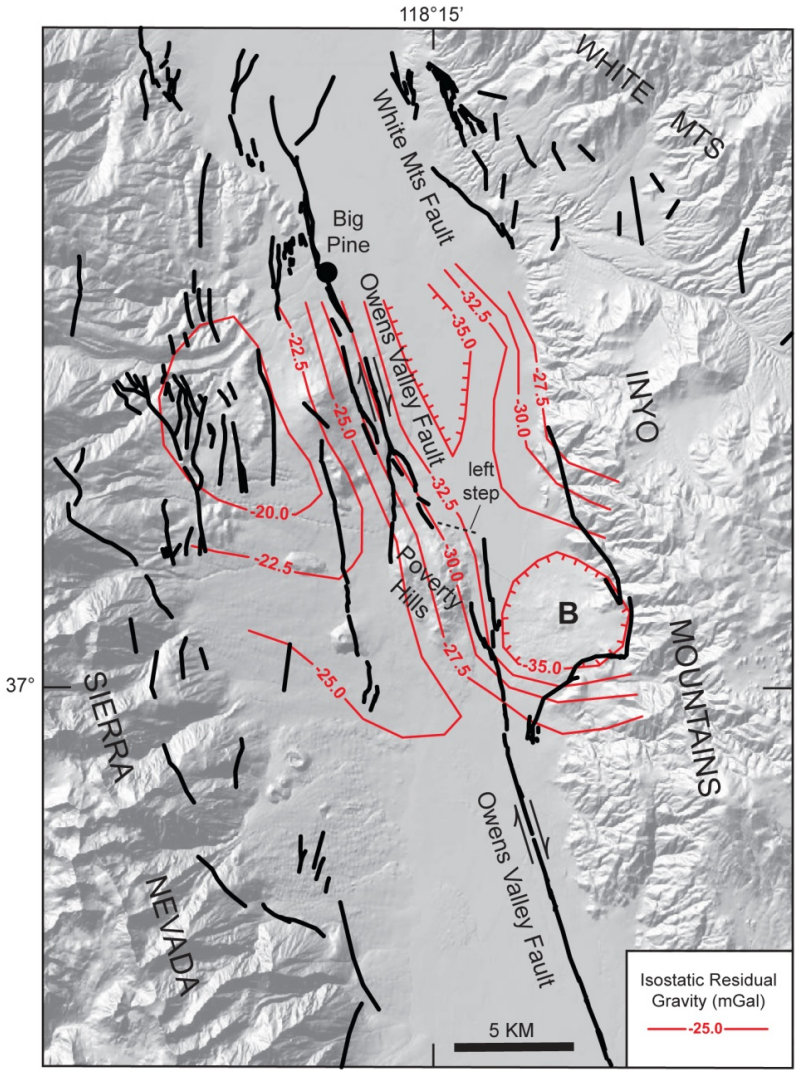

3. Major Structural Elements

Based largely on thickness variations of Cenozoic deposits and the positions of major faults (Figure 5), we divide the ESVS and the surrounding area into four major structural elements: (1) high, coherent mountain blocks that form the eastern and western boundaries of the ESVS (South Argus, North Argus, Inyo, and White Mountains blocks on the east and the Sierran Block on the west); (2) relatively high-standing, extended mountain blocks within the ESVS (Coso and Benton blocks); (3) relatively low-standing down-dropped blocks (North Argus, Independence, and North Bishop blocks); and (4) six deep structural basins (Indian Wells, Rose, Owens, Bishop, Chalfant, and Round Valley basins) (Figure 7). A seventh basin, the deep depression of the 0.76 Ma Long Valley Caldera [65], is structurally atypical of the ESVS and is not discussed in detail here.

For the purposes of this report, we treat the western bounding mountain block of the ESVS (Sierran Block) as a single, essentially continuous physiographic feature although we recognize that the southern part is broken by numerous extensional faults described in detail by Nadin and Saleeby [66] and Maheo *et al.* [67]. In contrast, the eastern boundary of the ESVS is structurally and physiographically divided into the four separate mountain blocks noted above (Figure 7).

The relatively high-standing, extended Coso and Benton blocks, which lie within the ESVS, are cut by numerous Quaternary faults (Figure 3) and are topographically lower than the coherent mountain blocks that bound the ESVS, although elevated relative to the deep basins and the down-dropped blocks. Both blocks consist of Mesozoic and older bedrock largely covered by Quaternary volcanic rocks. The Coso Block is bordered by the Northwest Argus Fault on the east, Rose Basin on the west, and the Argus Lineament and the Southern Inyo Structural Zone, features discussed below, on the south and north, respectively (Figure 7). Farther north the Benton Block is separated from the Sierran Block by Round Valley Basin and Long Valley Caldera, and from the White Mountains Block by Chalfant Basin (Figures 5 and 7).

The three relatively low-standing down-dropped blocks underlie parts of the modern topographic valleys that separate the coherent mountain blocks bordering the ESVS. We interpret the West Argus and Independence blocks (Figure 7) as large bedrock blocks that have been faulted down from the adjacent ranges, an interpretation supported by the gravity inversion (Figure 5) which shows rocks in both areas to be overlain by a relatively thin cover of sediment. The Independence Block, which includes exposed bedrock in the Alabama Hills, is bounded on the east by the largely dextral strike-slip Owens Valley Fault and on the west by the normal Independence Fault (Figure 3), the two together representing slip partitioning in the extant stress field [68]. The West Argus Block, which is completely covered by sediment *ca.* 1 km thick, is bounded on the east by the frontal fault of the Argus Range (SW Argus Fault), on the west by the Little Lake and Airport Lake faults (Figure 5), and on the north by the Argus Lineament (Figure 7). The smaller North Bishop Block, which essentially separates the deep Bishop and Chalfant basins (Figure 7), was first identified by Pakiser *et al.* [40] and has been interpreted by Hollett *et al.* [27] as a bedrock slump block with the top located *ca.* 400–450 m below the valley surface.

Figure 7. Map showing deep basins, relatively shallow down-dropped blocks, extended mountain blocks, and structural zones in the ESVS, which is bounded by largely unextended mountain blocks. CB = Chalfant Basin; NBB = North Bishop Block; RVB = Round Valley Basin.

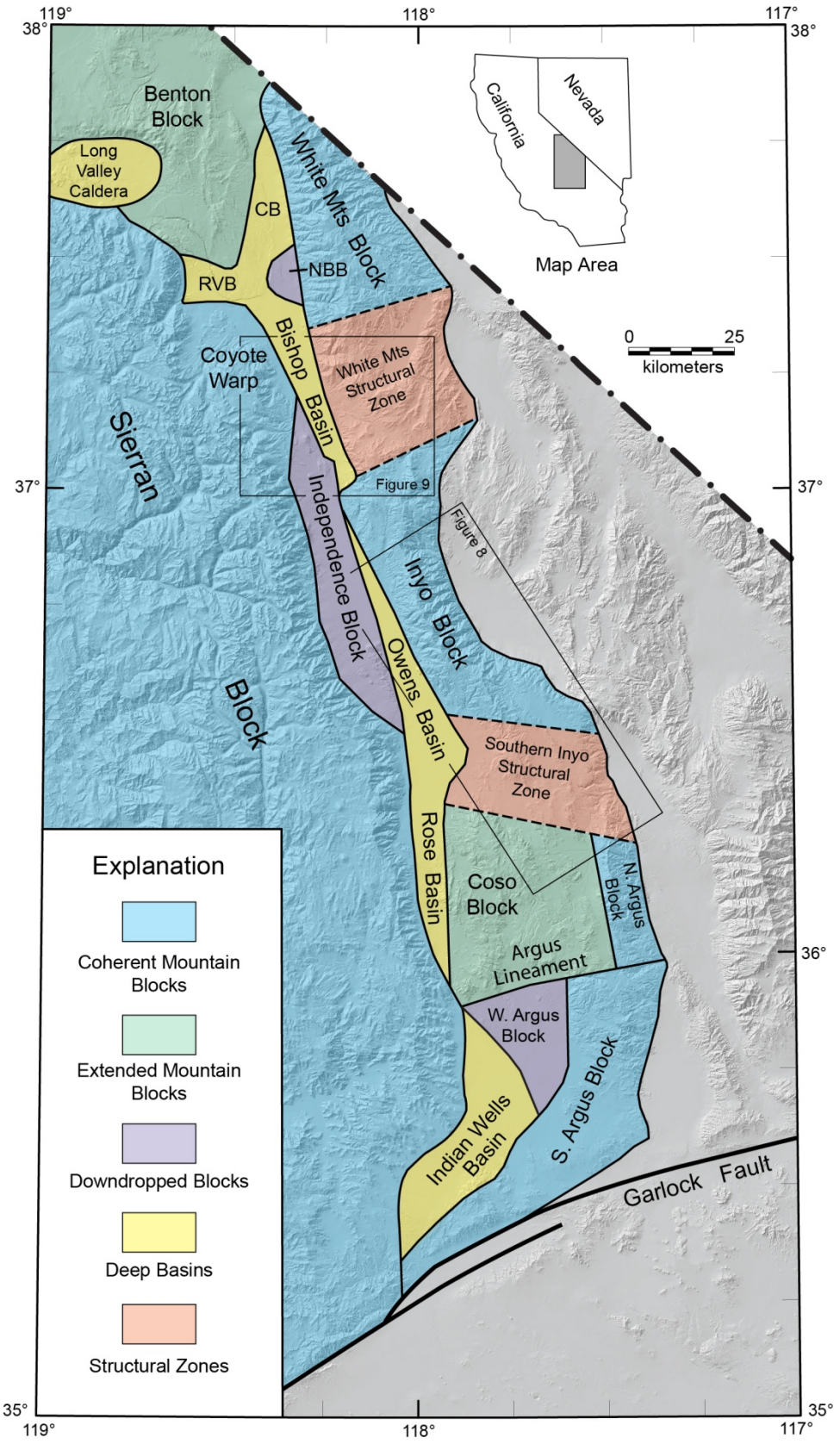

The deep structural basins have all been down-dropped along normal or oblique-slip faults. The Indian Wells Basin underlies the western part of Indian Wells Valley adjacent to the Sierran Block. Rose Basin lies in a narrow trough between the Sierran Block and the Coso Block, and much of the Owens Basin is sandwiched between the Inyo and Independence blocks. The Bishop and Chalfant basins lie immediately west of the White Mountains Block, and Round Valley Basin lies between the Benton and Sierran blocks (Figure 7).

4. Segmentation of the ESVS

We propose that the ESVS and the coherent mountain blocks to the east are latitudinally divided into four segments by three approximately east-west-oriented structural zones or boundaries that we call the Argus Lineament, the Southern Inyo Structural Zone (SISZ), and the White Mountains Structural Zone (WMSZ) (Figure 7). Although these structural zones or boundaries are defined primarily by bedrock relations in the mountain ranges east of the ESVS, they appear to be related to structural features in the ESVS itself and, locally, along the east side of the Sierran Block as well.

The Argus Lineament appears to be a very narrow structural boundary. This lineament bounds the Coso Range on the south and continues eastward where it forms the southern boundary of Darwin Wash. It also is marked by major canyons, one extending eastward and the other westward, in the Argus Range, and it bounds the northern end of the Slate Range and Searles Valley (Figures 2 and 7). The age and origin of the Argus Lineament are unknown. However, because this feature is not known to be the locus of Quaternary faulting, it probably represents an older fault on which no recent movement has been recognized.

The SISZ is marked primarily by an inferred major sinistral fault (here named the Santa Rosa Fault) which lies immediately south of the Santa Rosa Hills and the pre-Cenozoic bedrock of the Inyo Mountains (Figure 8). This fault, which has been interpreted to represent about 10 km of displacement [69], is overlain by Cenozoic basalt and alluvium. Drag on the Santa Rosa Fault has resulted in an eastward bend in the southern Inyo Mountains and a similar bend in the Santa Rosa Hills farther east (Figure 8). Probably associated with this eastward bend in the Inyo Mountains is a wide eastward bulge in the deep valley system at Owens Lake (Figure 5). The Darwin Fault, about 10 km to the south, which shows 1.6 km of sinistral displacement [69] (Figure 8), probably is also related to this deformation. As the Darwin Fault is partially buried [69] by 7.7 Ma basalt [70], it evidently is also inactive.

The WMSZ is a broad structural zone that we infer to separate the eastward-tilted White Mountains Block [22] from the westward-tilted Inyo Block to the south [24]. This difference in tilt direction seems to require the presence of an accommodation zone between the two ranges. Although such a structural zone has not been positively identified, the warping of bedding and fold hinges in Neoproterozoic and Cambrian strata from a northwesterly to a northeasterly trend across the Waucoba Embayment [71] (Figure 9) could have resulted from deformation between the two oppositely tilted structural blocks. We cannot be certain that this warping resulted from late Cenozoic deformation rather than from a much older event. However, the spatial proximity of this warping to the southern margin of Bishop Basin [27], the structural transition between the Independence Fault and the Coyote Warp at the eastern margin of the Sierra Nevada [54], and the Deep Springs Fault, which has accommodated eastward transfer of some right-lateral slip from the Owens Valley Fault to the Fish

Lake Valley Fault [47,48], suggests the possibility that all of these features (Figures 5 and 9) may be tectonically related.

Figure 8. Structural features defining the Southern Inyo Structural Zone (SISZ) [69,72]. Note bending in the southern Inyo Mountains and the Santa Rosa Hills. Strike and dip symbols indicate approximate bedding orientation. Dashes in Inyo Mountains extend trends through plutonic rocks. DF = Darwin Fault; SRF = Santa Rosa Fault.

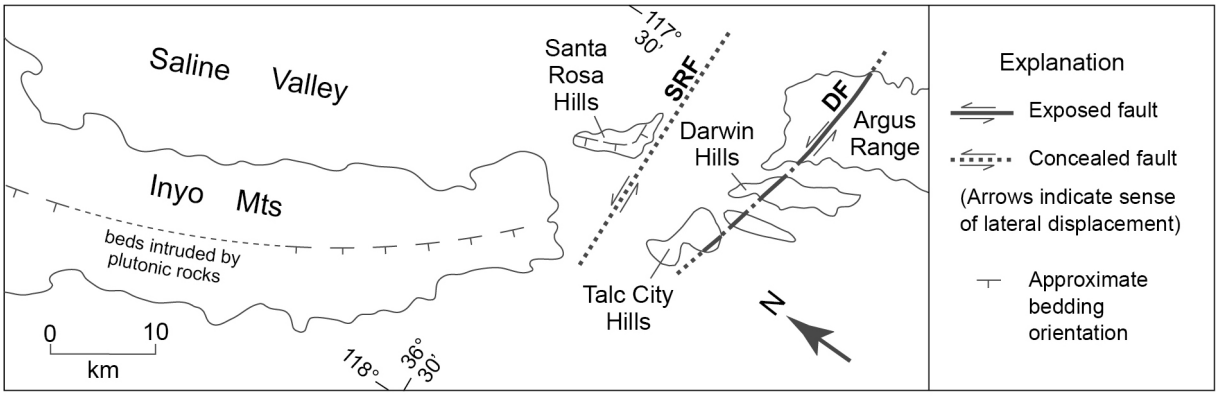

Figure 9. Geologic features in the White Mountains Structural Zone (WMSZ), including the Deep Springs Fault (DSF), the warping of bedding and folds across the Waucoba Embayment, the bight in the Inyo Mountains front (B), the southern boundary of the Bishop Basin, and the northward transition from the Independence Fault (InF) to the Coyote Warp [71,73]. OVF = Owens Valley Fault.

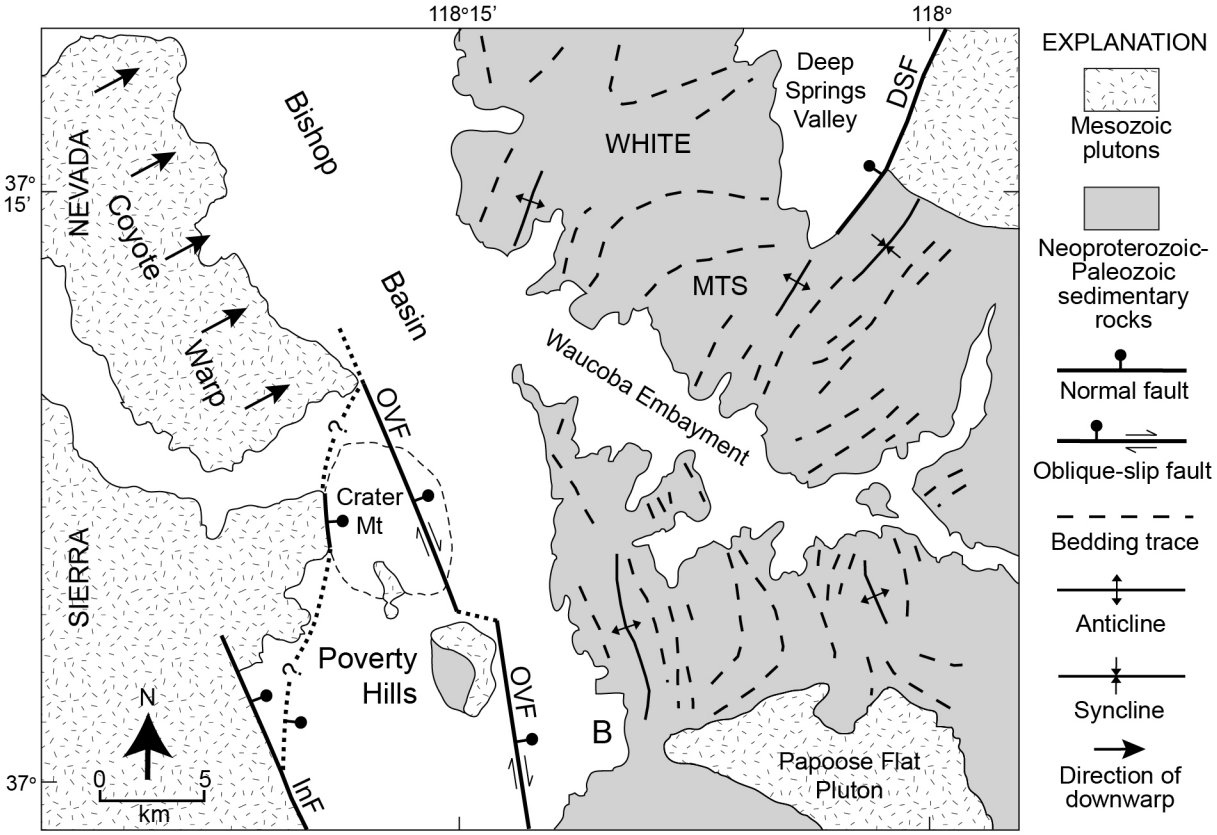

It is important to emphasize the interpretive and speculative nature of all three structural zones or boundaries, which are based primarily on general map relations in areas where changes in the basic structure of the mountain blocks and the adjacent valleys take place. Additional study along these zones would be necessary to elucidate the nature and significance of all the structural features involved.

Nevertheless these structural boundaries allow division of the ESVS into four segments. These are: (1) Indian Wells Basin and the West Argus Block; (2) Coso Block and Rose Basin; (3) Owens Basin and Independence Block; and (4) the Bishop, Round Valley, and Chalfant basins, and the North Bishop and Benton blocks. Here we describe and provide a brief geologic history of each segment based on a synthesis of gravity data (Figures 4 and 5) and previous studies. Structural cross sections and gravity profiles representing each part of the valley system are shown in Figure 10.

4.1. Indian Wells Basin and West Argus Block

Gravity data show that the subsurface Indian Wells Basin (Figures 4 and 5) is filled by a maximum of 2–3 km of sedimentary deposits. Drill-hole data [25] show that most of these deposits are late Miocene and younger, but that Paleocene and early to middle Miocene deposits are also present. The thickest Miocene-Pliocene section is in the western part of the basin, the margin of which is defined by the east-dipping Sierra Nevada frontal fault zone [25]. This fault zone is relatively steep at the surface, but seismic profiles show that the dip decreases to about 25° at depth [25] (Figure 10, A-A'). On the southeast the basin is bounded by the SW Argus Fault and on the northeast by the dextral Airport Lake Fault [44], which appears to connect northward with the dextral Little Lake Fault [74] (Figures 3 and 5).

Northeast across the Little Lake and Airport Lake faults, gravity data also indicate that bedrock in the eastern part of Indian Wells Valley is overlain by a relatively thin sedimentary cover. This area (West Argus Block, Figure 7) is down-faulted and down-bowed relative to the Argus Range to the east. Because gravity data suggest that the SW Argus Fault (Figure 5) accommodates only minor displacement, the overall subsurface geometry of Indian Wells Valley approximates that of a half-graben (Figure 10, A-A').

The Indian Wells Valley area has had a long and complicated history [25,75]. During the Paleocene, the area was the site of an east-west elongate basin in which nonmarine strata of the Goler Formation were deposited. Later, throughout most of the Miocene, the area was part of a large depositional basin in which volcanic rocks and sediments of the Ricardo Group accumulated. The Ricardo Basin originated prior to the *ca.* 10–11 Ma inception of movement on the left-lateral Garlock Fault [76], and was eventually transected by that fault. By late Miocene time (7–8 Ma), the Sierra Nevada had emerged as a sediment source area, and a northwest-trending extensional basin developed in the hanging wall of the east-dipping Sierra Nevada frontal fault zone. About 10 km of horizontal extension is estimated to have occurred across this basin between 7 and 3.5 Ma [25]. Since that time, the area has been characterized by right-lateral strike-slip faulting, with only minor continued movement on the Sierra Nevada frontal fault system.

Figure 10. Structural cross sections across the East Sierra Valley System (ESVS), with corresponding gravity profiles. Locations of sections are shown in Figure 5. No vertical exaggeration. Shading represents Quaternary sedimentary and volcanic deposits, with thicknesses based on inversion of gravity data [53]. Structural data from various sources [22,25,54,58,72,73,77–81].

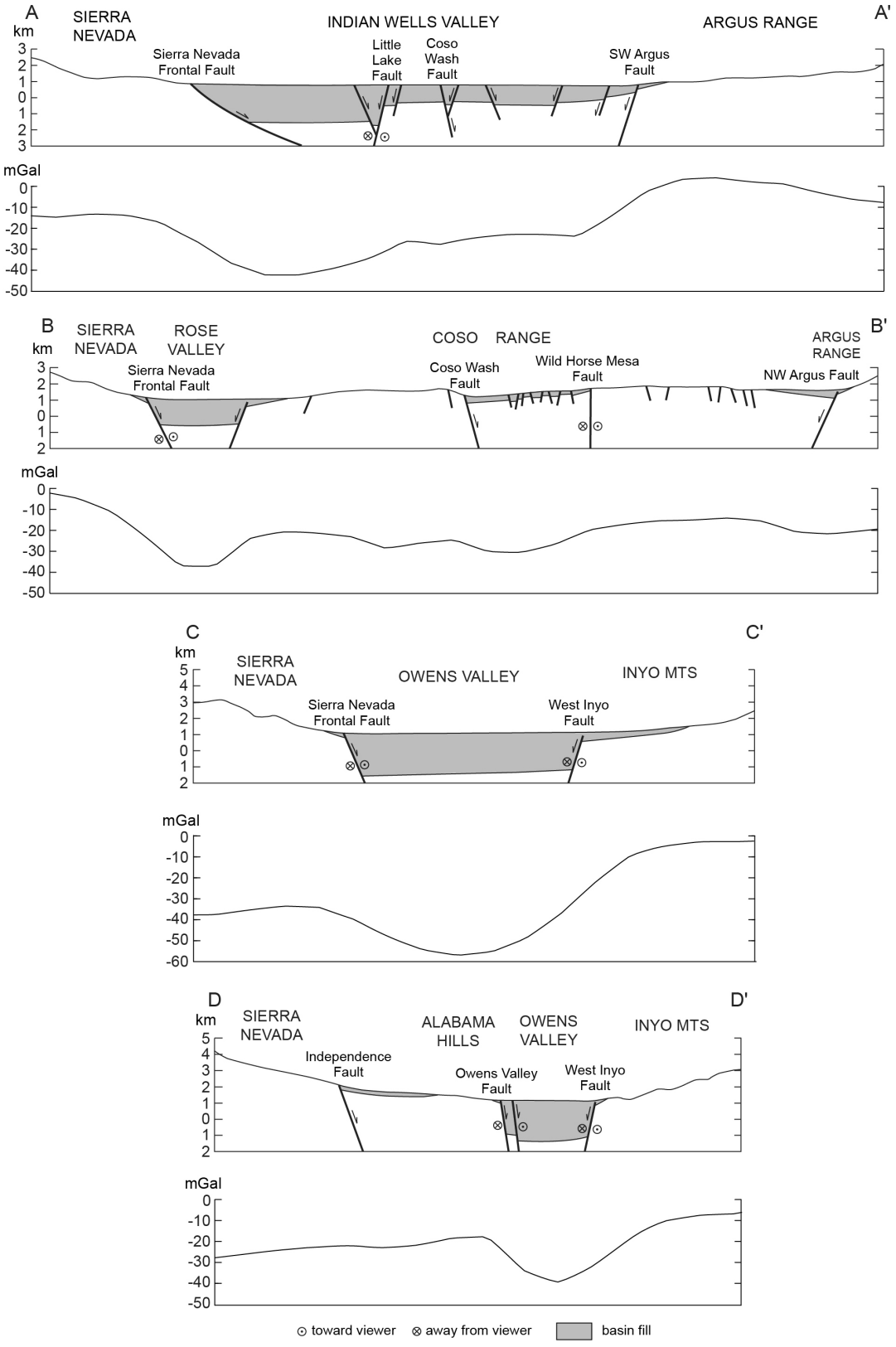

Figure 10. *Cont.*

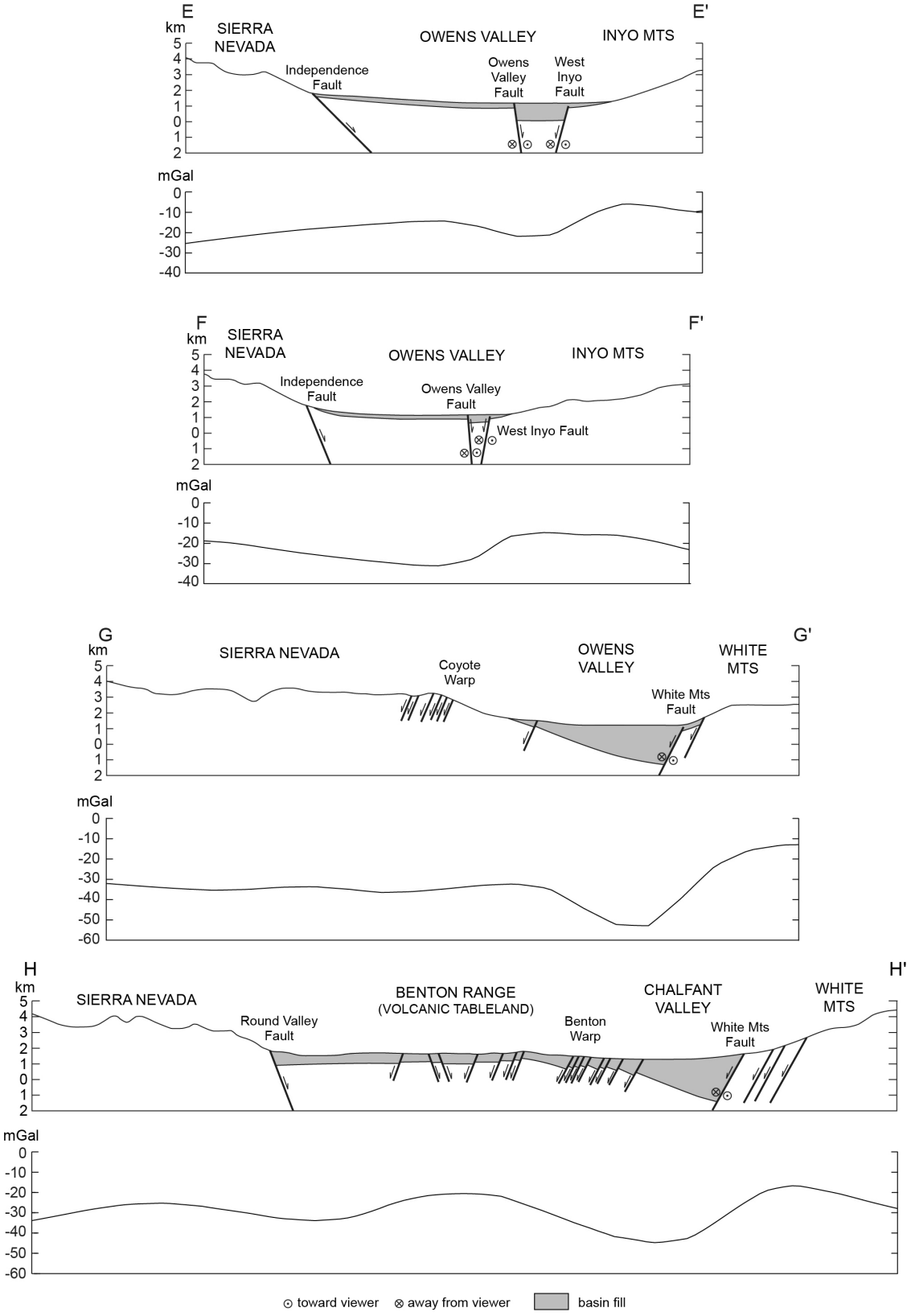

4.2. Coso Block and Rose Basin

The Coso Block can be characterized as an extended volcanic center that separates Indian Wells Valley from Owens Valley to the north (Figures 2 and 7). This block consists of pre-Cenozoic basement

rocks overlain by diverse volcanic and sedimentary deposits of late Miocene to Pleistocene age, including the Coso Formation [82–85]. The Coso Range, which contains a significant geothermal field and is an area of high seismicity and heat flow, is inferred to overlie a diapiric intrusive body at depth [26].

The southern boundary of the Coso Block is part of the prominent, east-west-trending Argus Lineament (Figure 7). To the north the block extends to the SISZ (Figures 7 and 8). The eastern margin of the block lies along the NW Argus Fault (Figures 5 and 7) where Miocene basalt has been down-dropped to the west on a series of step faults [17,86,87]. Rose Basin, which pinches out southward where the Coso Range impinges against the Sierra Nevada (Figures 5 and 7), marks the western boundary. Gravity data (Figures 4 and 5) show that Rose Basin contains as much as 2 km of sedimentary fill and suggest that the east side of the basin is bounded by a subsurface fault (Figure 10, B-B'). The inferred trace of this fault (Figure 5) is overlain by sedimentary and pyroclastic deposits of the Coso Formation [82]. This relation implies that the fault and most of the sedimentary fill in Rose Basin predate *ca.* 2.5 Ma, the approximate minimum age of the Coso Formation [85].

The Coso Block is cut by many north- to northwest-trending faults that represent significant Pliocene and younger extensional deformation, e.g., [51,83,86,88]. The amount of extension represented by these faults is uncertain, but Duffield *et al.* [83] noted that heat-flow anomalies such as that in the Coso Range imply an extension rate of about 10% per million years. Extension is especially notable in the vicinity of Coso Wash and Wild Horse Mesa, where a gravity low defines a shallow sedimentary basin (Figures 4 and 5). Pluhar *et al.* [58] interpreted this basin as a transtensional feature that developed between the right-lateral Little Lake and Wild Horse Mesa fault zones. Monastero *et al.* [26] have suggested that extension in this area is related to development of an incipient metamorphic core complex above a detachment system at a depth of 3–4 km.

According to Duffield and Roquemore [88] the area of the Coso Block was a terrane of gentle surface relief in the Pliocene. Jayko [17] interpreted the remnants of this surface as part of a regionally extensive, relatively flat erosion surface that had developed by the middle Miocene. As described by Jayko [17], this surface, now fragmented, can be traced both westward into the Sierran Block and eastward into the Argus Block. The Coso Block surface is topographically lower than those in the Argus and Sierran blocks, implying that the Coso Block has been relatively down-dropped. However, the Coso Block also has been uplifted recently relative to the surrounding basins, as shown by leveling and triangulation surveys near the center of the volcanic field [88], the basinward dips of Pliocene strata of the Coso Formation on the western and northern flanks of the Coso Range [82,89], and the southward dip of Pleistocene rocks along the southern flank [83].

We suggest that recent relative uplift of the Coso Block was related to emplacement of the underlying diapiric intrusion and development of the associated volcanic and geothermal center [26]. This interpretation is consistent with a structural model of Faulds and Varga (Figure 23B in [90]) that illustrates a close geometric relationship between normal faults and an underlying coeval pluton in the core of an extensional arch.

4.3. Owens Basin and Independence Block

The southern part of Owens Valley is underlain by the subsurface Owens Basin and the Independence Block (Figures 2 and 7). The Owens Basin is a deep structural trough bounded by the

Owens Valley Fault on the west and the West Inyo Fault to the east (Figures 3, 5, 7, and 10, C-C' to F-F'). West of the Owens Valley Fault, the Independence Block has been dropped down along the normal, east-dipping Independence Fault. The Independence and Owens Valley faults converge southward (Figure 3), and gravity data suggest that the two faults essentially merge into a single zone that extends along the Sierran front and connects with the Little Lake Fault farther south (Figure 5). We recognize that the youngest known surface trace of the Owens Valley Fault crosses the southern part of Owens Lake about 5 km east of the Sierran front and extends southward into the northernmost Coso Range where it evidently dies out [12]. However, we interpret the fault marked by this surface trace to be a minor branch of the master, basin-bounding fault zone to the west.

The seismically active Owens Valley Fault has a prominent surface trace that has been studied in detail by Beanland and Clark [8], who reported fault dips ranging from 66° W to 66° E. At depth, we infer that the fault generally dips steeply east toward the Owens Basin. The eastern boundary of the large gravity anomaly that we interpret to mark the West Inyo Fault along the Inyo Mountains (Figures 4 and 5) has no corresponding surface trace. We infer this fault to dip steeply west. An exposed fault showing evidence of late Quaternary right-lateral slip east of Owens Lake [91] may be a branch of the West Inyo Fault, although this exposed fault appears to have a component of normal movement with the east side down [92].

Owens Basin is widest and contains the greatest thickness of sediment at its south end where the Inyo Mountains front bends to the east (Figures 2 and 7). The sediment accumulation beneath Owens Lake is at least 3 km and possibly as much as 5 km thick (Figures 5 and 10, C-C') as estimated from inversion of gravity data [56]. Southward the Owens Basin continues along the Sierran front and is separated from Rose Basin (Figure 7) by a structural high along faults mapped by Jayko [86]. Northward the Owens Basin gradually decreases in both width and depth, ultimately pinching out near latitude 37° N where we infer that the Owens Valley and West Inyo faults effectively merge (Figures 5 and 10, D-D' to F-F').

Cored sediments beneath Owens Lake date back to *ca.* 0.8 Ma at a depth of *ca.* 320 m, including the 0.76 Ma Bishop Tuff at a depth of *ca.* 300 m [93]. This age-depth relation suggests that the oldest sediments in Owens Basin could be several million years old. Tilted and dissected fanglomerates of latest Miocene to Pliocene age have been documented on the west flank of the Inyo Mountains east of Owens Lake [94] and near Mazourka Canyon [95,96].

The evolution of the Owens Basin area probably dates back to the middle Miocene (*ca.* 15 Ma), when the Inyo Block is interpreted to have undergone rapid uplift and westward tilting along the East Inyo Fault (Figures 3 and 5) based on (U-Th)/He ages reported by Lee *et al.* [24]. This event predated alluvial-fan sedimentation on the east side of the Inyo Mountains that began around 13 Ma [35,94]. Lee *et al.* [24] suggested that normal slip on the Sierra Nevada frontal fault zone (Independence Fault; Figure 3) also could have begun more or less simultaneously with this deformation, with the west-tilted Inyo Block forming a half-graben in its hanging wall. Other studies, however, have presented evidence that much or all of the displacement on the Sierran frontal fault in this area must be significantly younger than 15 Ma (no earlier than 11 Ma according to Maheo *et al.* [97]). Alternatively, normal slip on the Owens Valley Fault rather than on the Independence Fault could have defined the western margin of the half-graben, or perhaps only a downwarped basin was developed at this time. In any case, the late Miocene to early Pliocene fanglomerates noted earlier could represent deposition near the eastern margin of this basin. Any sediments as old as middle Miocene, however, would have to lie buried in the deep subsurface.

The deep structural trough of Owens Basin probably developed since *ca.* 3 Ma, when the Inyo Block again experienced rapid uplift on the East Inyo Fault [24]. Normal faulting also likely was initiated on the West Inyo Fault (Figure 5) at this time, as indicated by the presence of numerous west-dipping normal faults that cut late Miocene to early Pliocene basalt on the west side of the Inyo Mountains [89,92]. Presumably, substantial vertical displacement in addition to the dominant right-lateral movement also took place on the Owens Valley Fault beginning around 3 Ma. Normal displacement on both the West Inyo and the Owens Valley faults appears to decrease northward to the point where these faults converge.

4.4. Bishop Basin and Vicinity

Bishop Basin extends from the latitude of the Poverty Hills and Tinemaha Reservoir northward to the vicinity of Bishop (Figures 2 and 7). This basin is bounded on the east by the White Mountains Fault and on the west by the Coyote Warp; no distinct frontal fault is thought to be present along this part of the Sierran margin. Gravity data suggest that the Bishop Basin is a half-graben, with the gently east-dipping surface of the Coyote Warp terminating at depth against the west-dipping White Mountains Fault (Plate 11 in [54]; Figure 10, G-G'). The boundary between Bishop Basin and Owens Basin to the south is an enigmatic, subsurface structural arch that was first recognized on the basis of gravity data by Pakiser *et al.* [40]. This structural arch has been discussed more recently by Hollett *et al.* [27], who interpreted it to be the result of faulting.

The sedimentary fill of Bishop Basin has a maximum thickness of at least 3 km (Figure 5). About 6 km southeast of Bishop, near the deepest part of the basin, the base of the Bishop Tuff lies at a depth of only about 200 m (Plate 7 in [54]), so much of the thick basin fill in this area must be significantly older. Dissected fanglomerate of late Pliocene to early Pleistocene age is exposed along the western front of the White Mountains [98], and farther south the early Pleistocene (2.0–2.2 Ma) Waucoba Lake Beds [99,100] crop out together with overlying fanglomerate in the Waucoba Embayment (Figure 2).

North of Bishop the deep basin system bifurcates, with the eastern valley continuing northward along the White Mountains Fault [22] (Figures 3 and 5). Normal faults dipping westward at about 60° characterize the southern part of the fault zone, whereas less steeply inclined dip-slip and right-lateral oblique-slip faults characterize the northern part [13]. To the west the Chalfant Basin separates the White Mountains Block from the Benton Block (Figure 7), which is highly faulted (Figures 3 and 10, H-H') and contains both metasedimentary and plutonic bedrock [77]. Bedrock of the Benton Block is overlapped by Quaternary volcanic rocks, including the Bishop Tuff, which erupted from Long Valley Caldera and forms Volcanic Tableland to the south (Figure 2). Gravity data indicate that the sedimentary fill in Chalfant Basin is more than 3 km thick, thinning northward to less than 200 m adjacent to the northern White Mountains (Figures 4 and 5). On the south, the down-dropped North Bishop Block lies between the deep Bishop and Chalfant basins (Figure 7).

The western arm of the bifurcated Bishop Basin extends northwestward from the southern end of Chalfant Valley to Round Valley Basin and ultimately to Long Valley Caldera (Figure 5). Round Valley Basin has been relatively down-dropped along the Sierra Nevada frontal fault system, here represented by the Round Valley Fault (Figure 2). Phillips and Majkowski [13] showed that the Round Valley Fault has an average eastward dip of *ca.* 40° and displays evidence of right-lateral displacement

in addition to the predominant normal displacement. Gravity data (Figures 4 and 5) suggest that Round Valley Basin is only moderately deep beneath the modern valley but deepens eastward to more than 3 km beneath the southern part of Volcanic Tableland. This basin beneath the Tableland connects northward with Chalfant Basin on the west side of the North Bishop Block. As previously noted by Pakiser *et al.* [40] and Pakiser and Kane (in [54]), both the northern and southern margins of the deep basin beneath Volcanic Tableland are apparently unfaulted based on the relatively gentle gravity gradients (Figures 4 and 5). The southern margin is part of the Coyote Warp, whereas the northern margin is defined by a structurally similar downwarp which we here call the Benton Warp (Figure 5). The eastern flank of the Benton Warp forms the western margin of Chalfant Basin.

In the area north of Bishop, extension between the Sierran and White Mountains blocks appears to be widely distributed. Chalfant Valley is interpreted to represent an active down-bowed block as suggested by the eastward tilt of the warped Bishop Tuff towards the White Mountains fault zone [13] (Figure 10, H-H'). We interpret the relatively high-standing Benton Block as a modestly extended bedrock block, similar to the Coso Block, and Round Valley Basin to represent additional extension at the eastern margin of the Sierra Nevada. Phillips and Majkowski [13] concluded that low-angle detachment faults are responsible for extension in this part of the ESVS and presented a favored model (their Figure 7C) of a west-dipping detachment at a depth of 4–7 km under the ESVS based on exposed low-angle normal faults and earthquake hypocenters.

The age of deformation that led to the development of Bishop Basin and the other structural features that characterize the northern part of Owens Valley is uncertain. Some interpretations are conflicting. For example, based primarily on the interpretation of apatite fission-track and (U-Pb)/Th thermochronologic cooling ages, Stockli *et al.* [22] concluded that major uplift and eastward tilting of the White Mountains Block on the White Mountains Fault took place as early as 12 Ma, and that relatively little additional uplift and tilting have occurred since 3 Ma. By contrast, Phillips *et al.* [101] presented evidence suggesting that eastward tilting of the Coyote Warp, which presumably was kinematically related to normal movement on the White Mountains Fault and development of the Bishop Basin half-graben (Figure 10, G-G'), largely postdated the eruption of 3.4-Ma basalt. Later deformation also is indicated by the structural position of the westward-dipping Waucoba Lake Beds which indicate at least 2 km of uplift of the White Mountains Block relative to Owens Valley since *ca.* 2 Ma [99]. In addition, Lueddecke *et al.* [98] inferred significant relative uplift of the White Mountains Block beginning about 3 Ma based on the age of the oldest known alluvial-fan deposits at the base of the range, and Phillips *et al.* [101] suggested a kinematic relationship between post-3.4 Ma development of the Coyote Warp and normal movement on the Round Valley Fault. Normal faulting and warping of the Bishop Tuff also indicate extensional deformation since 0.76 Ma [13].

Right-lateral slip is postulated to have initiated on the White Mountains Fault Zone *ca.* 3 Ma [22] and to have continued at a rate of about 1 mm/year [7] to the present, as indicated most recently by the 1986 Chalfant Valley earthquake which was produced by dominantly right-lateral slip on that fault [9].

5. Integrated Geologic History of the ESVS

As described above, the ESVS is a longitudinally segmented system of fault-bounded basins of diverse structural character and history. Although the ESVS is mainly a product of extensional

deformation since around 15 Ma with later right-lateral shear, earlier events in the region also played a significant role. Here we summarize the geologic history of the entire ESVS beginning with the Late Cretaceous.

5.1. Late Cretaceous to Middle Miocene Cooling, Exhumation, and Right-Lateral Strike-Slip Faulting

Late Cretaceous plutonism in the vicinity of the ESVS terminated around 80 Ma, e.g., [102]. Studies using apatite (U-Th)/He thermochronology have shown that rocks now exposed at high structural levels in both the Sierra Nevada and the White-Inyo Mountains cooled to temperatures corresponding to paleodepths of 2–3 km by *ca.* 55–75 and 53–58 Ma, respectively, ostensibly the result of erosional and/or tectonic exhumation [22,24,97,103,104]. Then, from Eocene to middle Miocene time, the ESVS region was characterized by slow denudation, crustal cooling, and development of a widespread erosional surface [17,22,24,104]. Phillips [28] suggested that by the middle Miocene the area of the present ESVS was a broad, low-relief upland.

As stated earlier, probably less than 10 km of the total 65 km of right-lateral offset interpreted to have occurred across the ESVS since the Late Cretaceous has taken place since early middle Miocene time [16]. Thus, at least 55 km of offset evidently took place on an older fault. Here we summarize the available evidence pertaining to the location, age, and tectonic significance of this older fault.

Evidence of large-scale right-lateral slip across the ESVS was first presented by Stevens *et al.* [34], who interpreted a displacement of 65 km based on offset between deposits in a Devonian submarine channel in the Inyo Mountains near Tinemaha Reservoir and in the Sierra Nevada near Mt. Morrison (Figure 2). They and later Stevens and Stone [105] inferred that this offset took place during the Triassic on the hypothetical Tinemaha Fault, which was postulated to extend northwestward between Tinemaha Reservoir and Mt. Morrison (Figure 11). The age of movement was based in part on the inferred location of the fault which passed through an area where the Late Triassic Wheeler Crest Granodiorite does not appear to be offset. More recently, however, 65 km of right-lateral offset also has been proposed to separate Late Cretaceous (83.5 Ma) dikes in the northern Coso Range and the coeval, petrologically similar Golden Bear Dike in the Sierra Nevada near Independence [15,16,106] (Figure 11). Because this offset presumably took place on the same fault as that which offset the Devonian channel deposits, the original location and age of the Tinemaha Fault are no longer tenable and are herein abandoned.

Thus, we now agree with Bartley *et al.* [16] that the offsetting fault most likely extended approximately north-south from Indian Wells Valley to Chalfant Valley and has been reactivated as the modern strike-slip fault system of the ESVS. This older fault, referred to here as the Tinemaha-proto Owens Valley Fault (T-pOVF, Figure 11), may be marked by ductile shear zones along the western fronts of the White Mountains, northern Inyo Mountains, and Coso Range [16]. A fault in this position accommodates the offset of the Devonian channel deposits while passing east of all outcrops of the Wheeler Crest Granodiorite. This fault also allows restoration of an apparent offset between archaeocyathid-bearing Cambrian rocks in the Benton Range [107] and farther south in the White Mountains.

As pointed out by Unruh *et al.* [3], the modern Owens Valley-White Mountains strike-slip fault system is unusual in that it strikes clockwise relative to the local northwestward motion of the Sierra

Nevada away from the North American craton. Therefore, this strike-slip fault system is thought to closely follow the original trace of the T-pOVF, which probably was at least partially controlled by the mechanical difference between rocks of the Sierra Nevada batholithic complex to the west and the predominant miogeoclinal sedimentary rocks to the east [16,106].

Figure 11. Map showing interpreted location of the Tinemaha-proto Owens Valley Fault (T-pOVF, solid line), which was later reactivated by the modern White Mountains, Owens Valley, and Little Lake fault zones. Dashed line = Tinemaha Fault of Stevens *et al.* [34] which is herein abandoned. Offsets of a Devonian channel [34] and the Coso-Golden Bear dikes [15] indicate a total of *ca.* 65 km of right-lateral displacement since late Cretaceous time. See text for further discussion.

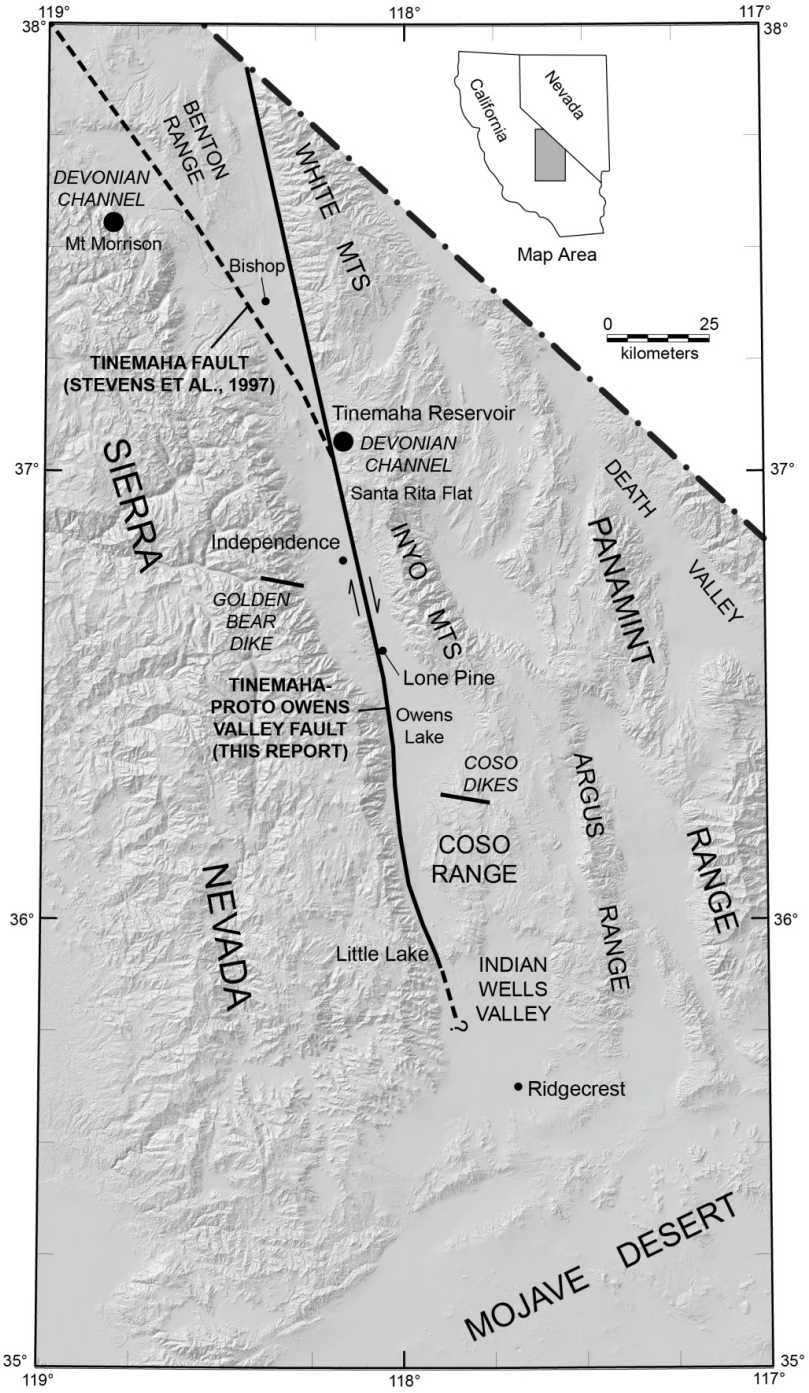

Bartley *et al.* [16] suggested that most of the lateral displacement on the T-pOVF took place in latest Cretaceous to Paleogene time in conjunction with Laramide unroofing of the southern Sierra Nevada on extensional faults [108,109]. By this interpretation, strike-slip faulting on both the T-pOVF and the proto-Kern Canyon fault, e.g., [66] would have accompanied the regional exhumation described above, as suggested by Lee *et al.* [24]. A strong component of right-lateral motion along the California continental margin between 80 and 56 Ma is allowed, although not required, by the plate tectonic reconstructions of Engebretson *et al.* [110].

Alternatively, as first noted by Kylander-Clark *et al.* [15], motion on the T-pOVF could have begun when the San Andreas Fault System started to develop in late Oligocene to early Miocene time. A hypothetical linear connection between the T-pOVF and the San Andreas Fault can be envisioned along the east side of the Sierra Nevada by restoring clockwise rotation of the southern Sierran tail (Figure 12). Some early San Andreas movement could have been accommodated on such a fault prior to 20 Ma, when rotation of the Sierran tail had been completed [111]. The apparent structural alignment of similar Paleozoic rocks in the southern Sierra Nevada and the El Paso Mountains [112], however, which would be on opposite sides of such a fault, argues against this hypothesis.

Figure 12. Map showing possible connection between the Tinemaha-proto Owens Valley Fault (T-pOVF) and the San Andreas Fault. T-pOVF could have originated as part of the early San Andreas Fault System prior to 20 Ma or older clockwise rotation of the southern Sierra Nevada.

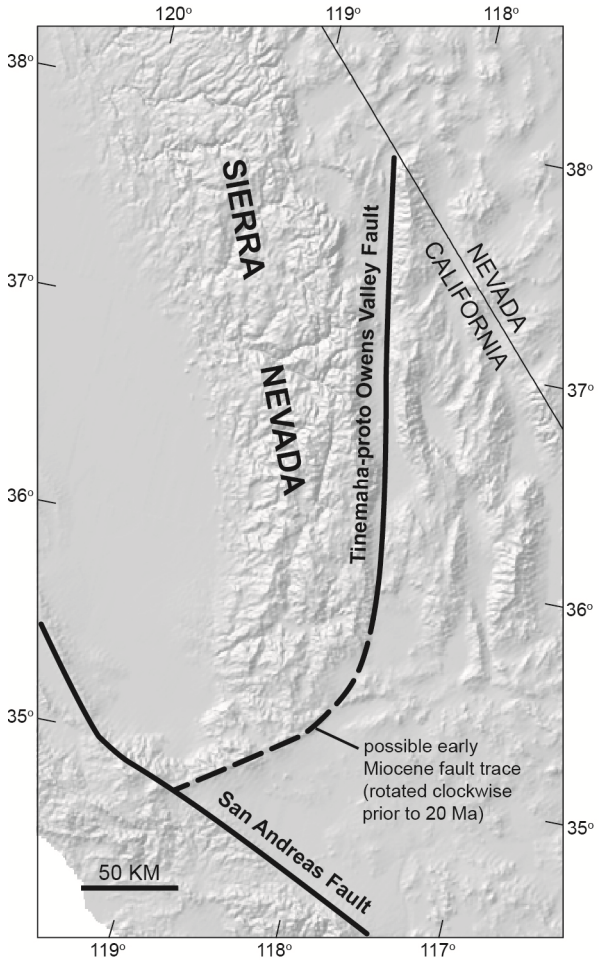

In summary, although timing of displacement on the T-pOVF is uncertain, it must have been sometime between the latest Cretaceous and early Miocene.

5.2. Middle Miocene to Early Pliocene Deformation

The widespread erosional surface that developed throughout the region in the early to middle Cenozoic was disrupted by westward tilting of the Sierra Nevada, possibly as early as 20 Ma [113]. Extensional faulting with relative uplift and westward tilting of the Inyo Block [24] probably started by *ca.* 15 Ma, followed by relative uplift and eastward tilting of the White Mountains Block possibly as early as 12 Ma [22]. As discussed earlier, we infer that this deformation produced half-grabens representing the initial stages of development of the Bishop Basin and possibly the Owens Basin. Any middle Miocene sediment deposited in these half-grabens, however, would now lie buried in the deep subsurface. We also infer that complex deformation in the White Mountains Structural Zone took place during this time to accommodate the opposing tilt directions of the Inyo and White Mountains blocks. Deformation associated with sinistral displacement on the Santa Rosa Fault in the Southern Inyo Structural Zone also may have originated at this time. Farther south, beginning around 7–8 Ma, Indian Wells Basin formed as another half-graben in the hanging wall of the Sierra Nevada frontal fault [25]. The tilted fault blocks that underlay all of these half-grabens may have been part of a Miocene breakaway zone extending northward into Nevada along the western margin of the Basin and Range Province [24].

During this phase of basin evolution, the Coso Block may have been differentiated from the subsiding Indian Wells Basin by faulting along the Argus Lineament. Most pre-Cenozoic bedrock in the Coso Block is overlain by volcanic or sedimentary deposits no older than *ca.* 4 Ma [83,84], suggesting that most parts of the block remained relatively high until at least that time. Farther north, the Benton Block, where no surficial deposits older than Quaternary are known, also probably remained structurally high relative to the adjacent subsiding basins.

Based on the above, we postulate that by late Miocene to early Pliocene time, the ESVS had evolved into a discontinuous series of half-grabens between the Sierra Nevada on the west and White-Inyo and Argus ranges on the east. Based largely on the apparent lack of extensive middle Miocene to early Pliocene deposits, Phillips [28] suggested that structural relief across Owens Valley by late Miocene to early Pliocene time was less than 1 km. Thermochronologic data, on the other hand, suggest that faulting could have created much greater structural relief across the valley by this time [22,24], and considerable thicknesses of early Pliocene and older sediments could be concealed beneath the present valley floor. Farther south, as much as 2 km of sediment was deposited in the Indian Wells Basin half-graben during late Miocene to early Pliocene time [25], confirming contemporaneous structural relief of at least this magnitude.

Middle Miocene to early Pliocene deformation in the ESVS was broadly coeval with major extensional deformation documented farther east. According to Andrew and Walker [114], faults in the Panamint Valley region they called the Emigrant, Panamint and Slate Range detachments were parts of a single normal fault at *ca.* 15 Ma which was then rotated to lower dips. They also pointed out that a change from extension to transtension progressed from Death Valley at 11 Ma, to Panamint Valley after 4.6 Ma, and finally to Owens Valley at 2.8 Ma. In addition, the central Panamint Range is thought to

have been structurally unroofed by pre-11 Ma extensional faulting along the Harrisburg detachment [115], and east of Death Valley, the Black Mountains were unroofed by extensional faulting on the Amargosa detachment between 9 and 5 Ma [2]. The detachment faults involved in these events must have extended westward in the subsurface toward the ESVS and could have played a role in the coeval extensional deformation there, although no direct link has been established. Late Miocene (7–8 Ma) extensional deformation also has been documented on the Darwin Plateau [70], between the Inyo Mountains and the Argus Range (Figure 2).

5.3. Late Pliocene to Recent Deformation

Events leading to development of the deep basin system that characterizes the modern ESVS probably began in late Pliocene time, in conjunction with initiation of a transtensional structural regime [28]. In the southern part of the ESVS, right-lateral oblique slip on the Little Lake and Airport Lake faults beginning *ca.* 3.5 Ma [25] apparently controlled deepening of the Indian Wells Basin immediately to the west. Farther north, normal faulting between *ca.* 4 and 2.5 Ma led to the formation of Rose Basin prior to deposition of the youngest beds of the Coso Formation, as inferred from gravity data discussed previously in this paper. At about the same time, renewed tilting of the Inyo Block *ca.* 3 Ma [24] and post-4 Ma normal faulting on the west side of this block [92] were clearly related to deepening of the Owens Basin. Right-lateral oblique slip on the Owens Valley Fault, which forms the western boundary of the deep Owens Basin, presumably also was initiated at about the same time, although this cannot be conclusively demonstrated based on existing data.

As these deep basins formed, the adjacent Coso Block was experiencing a complex history. The presence of a thin cover of Pliocene to Pleistocene sedimentary and volcanic deposits in this block suggests a period of modest subsidence approximately coeval with downfaulting of the surrounding basins. Later the Coso Block was evidently uplifted in response to magmatic processes that led to development of the Quaternary volcanic and geothermal center [83].

In the northern part of the ESVS, the Bishop and Chalfant basins probably were significantly deepened when the White Mountains Fault was reactivated as a right-lateral oblique-slip fault *ca.* 3 Ma [22]. This faulting was presumably coupled with eastward tilting of the Coyote Warp [101] and the structurally similar Benton Warp to the north (Figure 5). The structure and position of the Waucoba lake beds reflect 6° of westward tilting and more than 2 km of uplift of the White-Inyo Mountains relative to Owens Valley since *ca.* 2 Ma [99].

Late Pliocene and younger transtensional deformation was also widespread in the region directly east of the ESVS, resulting in the opening of Panamint, Saline, and Eureka valleys, e.g., [2,4,116,117] (Figures 2 and 5). Northern Panamint Valley, which has been extensively investigated [117,118], is especially relevant to our study. It is a pull-apart basin underlain by a low-angle detachment fault which surfaces as the Panamint Valley Fault to the east and southeast (Figures 3 and 5). Burchfiel *et al.* [117] placed the dip of the detachment at 0°–15° west and showed that movement on this fault postdated eruption of basalt dated *ca.* 4 Ma. MIT 1985 Field Geophysics Course and Biehler [118], based on detailed geophysical work, placed the detachment at 1.7 ± 1.2 km below the playa in the northern Panamint Valley, which is at an elevation of about 0.5 km above sea level. Thus, the detachment there apparently lies between sea level and about 2.5 km below it.

This detachment surface, which Andrew and Walker [114] called the Panamint Detachment, extends beneath the Darwin Plateau (Figure 2) and is not known to surface to the west. Wesnousky and Jones [68] therefore suggested that the detachment extends beneath the southern Inyo Mountains and part of Owens Valley. Earlier, Hamilton [119] had suggested that the Argus Range also is underlain by a detachment fault at a shallow depth and postulated that this range may have lain above the Panamint Range prior to extension. Cichanski [120] has shown that some low-angle faults on the west side of the Panamint Range are cut by high-angle faults showing right-lateral displacement, suggesting that currently these low-angle faults are dormant. However, the low-angle surface described by Numelin *et al.* [121], also on the west side of the Panamint Range, apparently indicates active deformation, a view concurred with by Andrew and Walker [114] who indicated that there is continuing oblique-slip on low-angle faults in Panamint Valley. These studies thus suggest that these faults are related to the Panamint Detachment, which likely extends beneath at least the southern Inyo Mountains and the entire Argus Range.

Extension is transferred northward from Panamint Valley to Saline Valley on the dextral Hunter Mountain Fault [117] (Figure 5). The structural continuity of the Inyo Mountains west of the termination of the Hunter Mountain Fault (Figure 5) seems to require the Panamint Detachment to extend beneath this entire range. By this interpretation, the Argus and Inyo Mountains overlie a common detachment fault which surfaces just east of the Panamint and Saline-Eureka valleys. Extension north and south of the Hunter Mountain Fault, however, is evidently accommodated differently. In Panamint Valley, extension is taken up by a single detachment fault, whereas in Saline Valley extension probably is taken up by closely spaced, rotated normal faults that merge into the detachment surface at depth [117]. Because gravity data show that Saline Valley and the contiguous Eureka Valley to the north contain more than 3 km of sedimentary and volcanic material [116] (Figures 4 and 5), the detachment surface beneath these valleys apparently is deeper than beneath the relatively shallow Panamint Valley. This difference could be caused by steeper fault dips along the breakaway zone of the detachment surface on the east sides of Saline and Eureka Valleys than on that of Panamint Valley.

If the Panamint Detachment underlies the Argus Range and the entire Inyo Mountains, it very likely extends northward beneath the structurally contiguous White Mountains as well. Thus we envision the Argus and White-Inyo ranges moving away from the ranges to the east on an underlying detachment fault, which although probably complex in detail, is an essentially continuous surface dipping gently westward under the ESVS.

We illustrate this concept in an interpretive cross section extending from the Panamint Range westward to the Sierra Nevada through Owens Lake (Figures 2 and 13). This cross section shows the Panamint Detachment dipping gently west beneath the southernmost Inyo Mountains where it intersects the more steeply west-dipping West Inyo Fault at the eastern margin of Owens Valley. The depth of such an intersection is speculative, but we place it at about 5 km below sea level based on a 10° dip of the Panamint Detachment, well within the limits suggested by Burchfiel *et al.* [117]. At the point of intersection, we show the two faults merging into a single fault that continues westward at an intermediate dip. We infer that both the merged west-dipping fault and the east-dipping Sierra Nevada frontal fault extend downward into the brittle-ductile transition zone below a depth of *ca.* 10 km [19,20,41], where they pass into a zone of horizontal ductile extension and shear. Other, structurally lower

detachment faults, such as the Amargosa Detachment [115], may extend westward from the Death Valley area and may terminate in the brittle-ductile transition zone east of the ESVS (Figure 13), although Norton [122] argued that the Amargosa Detachment actually extends above the Panamint Range. Regardless, the Amargosa Detachment apparently is older than the Panamint Detachment.

Figure 13. Cross section X-X' (Figure 2) illustrating possible structure of the Owens Valley transtensional graben. Horizontal arrows represent ductile extension below Owens Valley. See text for further discussion. SNFF, Sierra Nevada Frontal Fault; TPF, Towne Pass Fault; WIF, West Inyo Fault. No vertical exaggeration.

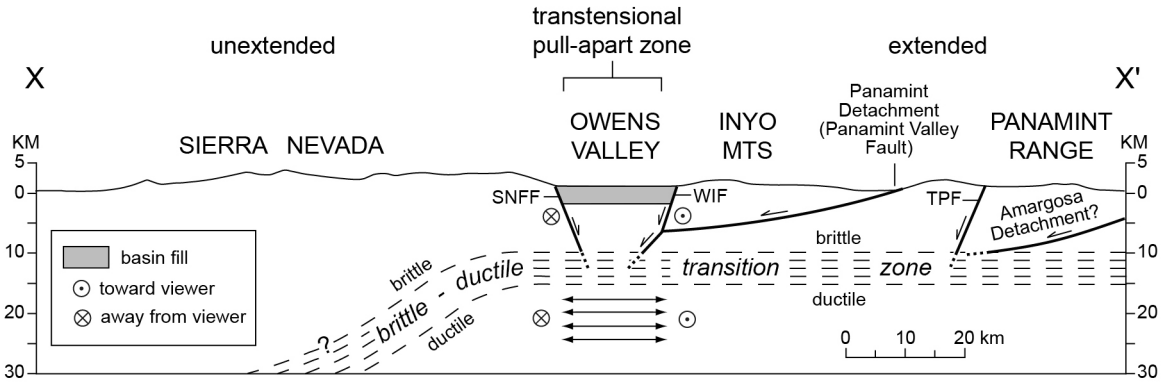

6. Discussion

Our conclusions regarding the tectonic development of the ESVS are similar to those proposed by Blakely *et al.* [55] for the development of Death Valley. Both valley systems apparently originated as a result of east-west extension in middle to late Miocene time and were later modified by right-lateral oblique extension that continues to the present. Based on gravity data, Blakely *et al.* [55] demonstrated that Death Valley is underlain by four deep (3–5 km), steep-sided depressions that may have formed as transtensional pull-apart basins superimposed on the earlier, more uniform extensional valley. The geometrically similar deep basins of the ESVS may have formed in much the same way.

Extension in the central Basin and Range Province began around 16 Ma as the Sierra Nevada-Great Valley microplate (SN-GVm) began to move relatively westward away from the Colorado Plateau [1,2,4]. Although extension from *ca.* 16–10 Ma was largely concentrated between the Colorado Plateau and the Spring Mountains (Figure 1), some extension was also occurring farther west. Initial development of the East Sierra Valley System (ESVS) during this time interval, for example, indicates that the SN-GVm was already beginning to break away from the structural blocks directly to the east. Since 8–10 Ma, when the relative movement of the SN-GVm changed to northwesterly, extension and right-lateral strike-slip faulting have been concentrated largely west of the Spring Mountains (Figure 1). The modern ESVS has resulted from right-lateral oblique extension since ~3 Ma as the SN-GVm pulled farther away from the White-Inyo-Argus structural blocks to the east.

The deep basins of the ESVS apparently developed more or less simultaneously with uplift of the Sierra Nevada. Several recent studies have concluded that this uplift was induced by Pliocene detachment and sinking of the dense eclogitic root of the Sierran batholith, e.g., [32,123]. Another concept was presented by Jayko and Bursik [14] and Jayko [18], who proposed that the Sierra Nevada

was uplifted as part of a broad topographic flexure (Mono Arch) that rose in response to mantle upwelling beginning in the late Miocene. In contrast**,** some authors, e.g., [124,125] have rejected the inference that the Sierra Nevada has been elevated since the late Miocene based on deuterium and oxygen isotopic studies. Molnar [126], however, has interpreted their data as consistent with a rise of the Sierra Nevada of 1 km or more since the late Miocene, and a recent analysis of low-temperature thermochronology [113] indicates 2 km of surface uplift since 20 Ma. Based on GPS and InSAR measurements, Hammond *et al.* [21] have shown that vertical motion of the Sierra Nevada relative to stable eastern Nevada is presently occurring at a rate between 1 and 2 mm/year.

Our structural model of the ESVS (Figure 13) implies a kinematic link between the high-angle faults that bound the ESVS and low-angle, west-dipping detachment faults that are interpreted to underlie the White, Inyo, and Argus ranges. After about 3–3.5 Ma we envision both fault systems to have experienced displacement simultaneously in response to movement of the SN-GVm away from the crustal blocks directly to the east. Our structural model also infers that displacements on faults in the brittle upper crust pass downward into ductile shear in the middle crust, below a depth of *ca.* 10 km.

We interpret the Panamint Detachment to underlie not only the Argus Block and the southern Inyo Block, but also the White Mountains Block and the ESVS. This interpretation is somewhat similar to that of Phillips and Majkowski (Figure 7C in [13]), who postulated a detachment surface below the Bishop Basin. However, in contrast to Phillips and Majkowski [13], we do not interpret any major detachment faults to extend westward beneath the Sierra Nevada. Instead, we envision the extensional fault system to end within the ESVS, except locally where down-dropped blocks along the eastern margin of the SN-GVm, such as the Independence and Benton blocks, are being incorporated into the Basin and Range structure.

We interpret the SN-GVm to be a thick, largely unextended lithospheric microplate that has moved away from the North American craton in response to continental rifting. In many ways the SN-GVm resembles Baja California as described by Faulds and Henry [6] and Umhoefer [29], and the present character of the ESVS resembles that of the proto-Gulf of California at 12–6 Ma [6]. Both the SN-GVm and Baja California consist primarily of strong batholithic rocks, have similar directions of displacement away from cratonal North America, and have rift zones along their eastern margins (the ESVS and the Gulf of California, respectively) characterized by dextral shear oriented at an angle to the direction of plate motion. Fletcher [30] has pointed out that such orientations are common and are the result of thermal or mechanical weaknesses. In the Gulf of California rifting took place along a Miocene volcanic arc with an extensional backarc basin located between two strong batholiths [29]. In the ESVS an old break (the T-pOVF) along the margin of the strong Sierra Nevada composite batholiths localized regional deformation. The histories of these two systems also are similar. The ESVS probably originated as part of a broad system of extension in the middle to late Miocene followed later by dextral shearing. Similarly, the Gulf of California was initiated by mid-Miocene rifting and extension [127] followed by progressive localization of dextral shear beginning at least by 6 Ma [29] or *ca.* 7 Ma [128]. Finally, as indicated by Martin *et al.* [129], extension in the northern Gulf of California is accommodated on a series of listric-normal faults that merge at depth into a detachment similar to that proposed here for the structure of the ESVS.

A major difference between the two extensional systems is that the Gulf of California shows active spreading and development of oceanic crust whereas the ESVS has not fully ruptured, e.g., [6]. Thus,

the Gulf of California is more highly developed than the ESVS. It is conceivable that in the future the ESVS may develop into a rift system similar to the Gulf of California and the SN-GVm may eventually dissociate from cratonal North America [6]. If almost 50% of the present motion along the Walker Lane continues to be localized on the Little Lake/Airport Lake fault system, as reported by McClusky *et al.* [130], the eastern boundary of the allochthonous SN-GV microplate in the future probably will be marked by the Airport Lake-Little Lake-Owens Valley fault zone [131].

7. Summary

The East Sierra Valley System (ESVS), composed of the Indian Wells, Rose, Owens, Chalfant, Round, and Long valleys, marks the western limit of the Basin and Range Province. Although this area is currently very active tectonically, the geologic history leading up to its present structure and morphology is long and complex. Four major events are recognized: (1) Late Cretaceous–early Cenozoic, post-batholithic exhumation of the ESVS region, followed by development of a broad denudational surface of low relief prior to the middle Miocene; (2) development of a major right-lateral fault zone (Tinemaha-proto Owens Valley Fault, or T-pOVF) that accommodated *ca.* 55 km of displacement sometime between the Late Cretaceous and early Miocene; (3) middle Miocene to early Pliocene extension and development of the incipient ESVS as a system of tilted fault blocks and half-grabens; and (4) late Pliocene to Recent right-lateral oblique extension that led to displacement on steeply-dipping faults that bound the modern ESVS and low-angle detachment faults that underlie it and the White, Inyo, and Argus ranges and surface to the east.

The ESVS is not a simple graben but a complex, longitudinally segmented system of diverse structural and morphological elements including deep sedimentary basins, relatively low-standing down-dropped blocks, and relatively high-standing extended blocks, all of which lie between bounding high, largely unextended mountain blocks. Isostatic gravity anomalies clearly depict the deep basins and enhance our ability to interpret the structural framework of the valley system. The modern dextral strike-slip fault system that characterizes the ESVS represents reactivation of the old T-pOVF, probably accommodating a maximum of about 10 km of lateral displacement since late Pliocene time.

The modern ESVS began to form when the Sierra Nevada-Great Valley microplate (SN-GVm) started moving relatively westward away from cratonal North America in middle Miocene time, and attained its present structure as a result of northwestward relative movement of the SN-GVm away from the White, Inyo, and Argus mountain blocks beginning in the late Pliocene. Uplift of the Sierran Block since about 3 Ma may have taken place in response to detachment and sinking of the deep eclogitic root of the Sierra Nevada batholith. Continued rifting in the ESVS could lead to complete rupture between the SV-GSm and cratonal North America and creation of narrow ocean basin comparable to the Gulf of California.

Acknowledgments

Reviews by J.M. Bartley and two anonymous reviewers led to substantial improvements in the manuscript. Reviews of earlier versions of the manuscript by C.B. Amos, C.J. Busby, K.A. Howard, J.W. Hillhouse, R.B. Miller, F.M. Phillips, and K.D. Putirka are also appreciated. Finally, our work has

benefited from discussions with several additional colleagues including K.M. Bishop, J.P. Colgan, A.S. Jayko, and A.C. Robinson.

References

1. Wernicke, B.; Snow, J.K. Cenozoic tectonism in the central Basin and Range: Motion of the Sierran-Great Valley Block. *Int. Geol. Rev.* **1998**, *40*, 403–410.
2. Snow, J.K.; Wernicke, B.P. Cenozoic tectonism in the central Basin and Range: Magnitude, rate, and distribution of upper crustal strain. *Am. J. Sci*. **2000**, *300*, 659–719.
3. Unruh, J.; Humphrey, J.; Barron, A. Transtensional model for the Sierra Nevada frontal fault system, eastern California. *Geology* **2003**, *31* (4), 327–330.
4. McQuarrie, N.; Wernicke, B.P. An animated tectonic reconstruction of southwestern North America since 36 Ma. *Geosphere* **2005**, *1* (3), 147–172.
5. Wernicke, B.; Davis, J.L.; Niemi, N.A.; Luffi, P.; Bisnath, S. Active megadetachment beneath the western United States. *J. Geophys. Res*. **2008**, *113*, B11409:1–B11409:26.
6. Faulds, J.E.; Henry, C.D. Tectonic influences on the spatial and temporal evolution of the Walker Lane: An incipient transform fault along the evolving Pacific-North American plate boundary. In *Ores and Orogenesis: Circum-Pacific Tectonics, Geologic Evolution, and Ore Deposits*; Arizona Geological Society Digest 22; Spencer, J.E, Titley, S.R., Eds.; Arizona Geological Society: Tucson, AZ, USA, 2008; pp. 437–470.
7. Dixon, T.H.; Miller, M.; Farina, F.; Wang, H.; Johnson, D. Present-day motion of the Sierra Nevada block and some tectonic implications for the Basin and Range province, North America Cordillera. *Tectonics* **2000**, *19* (1), 1–24.
8. Beanland, S.; Clark, M.M. *The Owens Valley Fault Zone, Eastern California, and Surface Faulting Associated with the 1872 Earthquake*; U.S. Geological Survey Bulletin 1982; U.S. Government Printing Office: Washington, DC, USA, 1994.
9. Savage, J.C.; Gross, W.K. Revised dislocation model of the 1986 Chalfant Valley earthquake, eastern California. *Bull. Seismol. Soc. Am*. **1995**, *85(2)*, 629–631.
10. Gillespie, A.R. Quaternary subsidence of Owens Valley, California. In *Natural History of Eastern California and High-Altitude Research (White Mountain Research Station Symposium)*; Hall, C.A., Jr., Doyle-Jones, V., Widawski, B., Eds.; University of California White Mountain Research Station: Los Angeles, CA, USA, 1991; Volume 3, pp. 356–382.
11. Lee, J.; Spencer, J.; Owen, L. Holocene slip rates along the Owens Valley Fault, California: Implications for the recent evolution of the Eastern California Shear Zone. *Geology* **2001**, *29* (9), 819–822.
12. Slemmons, D.B.; Vittori, E.; Jayko, A.S.; Carver, G.A.; Bacon, S.N. *Quaternary Fault and Lineament Map of Owens Valley*, *Inyo County*, *Eastern California*; Geological Society of America Map and Chart Series MCH096; Geological Society of America: Boulder, CO, USA, 2008; Scale 1:100,000.
13. Phillips, F.M.; Majkowski, L. The role of low-angle normal faulting in active tectonics of the northern Owens Valley, California. *Lithosphere* **2008**, *3* (1), 22–36.

14. Jayko, A.S.; Bursik, M. Active transtensional intracontinental basins: Walker Lane belt in the western Great Basin. In *Tectonics of Sedimentary Basins: Recent Advances*; Busby, C., Perez, A.A., Eds.; Wiley-Blackwell: Chichester, UK, 2012; pp. 226–248.
15. Kylander-Clark, A.R.C.; Coleman, D.S.; Glazner, A.F.; Bartley, J.M. Evidence for 65 km of dextral slip across Owens Valley, California since 83 Ma. *Geol. Soc. Am. Bull*. **2005**, *117* (7/8), 962–968.
16. Bartley, J.M.; Glazner, A.F.; Coleman, D.S.; Kylander-Clark, A.R.C.; Mapes, R.; Friedrich, A.M. Large Laramide dextral offset across Owens Valley, California, and its possible relation to tectonic unroofing of the southern Sierra Nevada. In *Exhumation Associated with Continental Strike-Slip Fault Systems*; Geological Society of America Special Paper 434; Till, A.B., Roeske, S.M., Foster, D.A., Sample, J.C., Eds.; Geological Society of America: Boulder, CO, USA, 2007; pp. 129–148.
17. Jayko, A.S. Deformation of the late Miocene to Pliocene Inyo Surface, eastern Sierra region, California. In *Late Cenozoic Structure and Evolution of the Great Basin-Sierra Nevada Transition*; Geological Society of America Special Paper 447; Oldow, J.S., Cashman, P.H., Eds.; Geological Society of America: Boulder, CO, USA, 2009; pp. 313–350.
18. Jayko, A.S. The Mono Arch, eastern Sierra region, California: Dynamic topography associated with upper-mantle upwelling? *Int. Geol. Rev*. **2009**, *51* (7/8), 702–722.
19. Savage, J.C.; Lisowski, M. Strain accumulation in Owens Valley, California, 1974 to 1988. *Bull. Seismol. Soc. Am.* **1995**, *95* (1), 151–158.
20. Dixon, T.H.; Norabuena, E.; Hotaling, L. Paleoseismology and global positioning system: Earthquake-cycle effects and geodetic *versus* geologic fault slip rates in the Eastern California Shear Zone. *Geology* **2003**, *31* (1), 55–58.
21. Hammond, W.C.; Blewitt, G.; Li, Z.; Plag, H.-P.; Kreemer, C. Contemporary uplift of the Sierra Nevada, western United States, from GPS and InSAR measurements. *Geology* **2012**, *40* (7), 667–670.
22. Stockli, D.F.; Dumitru, T.A.; McWilliams, M.O.; Farley, K.A. Cenozoic tectonic evolution of the White Mountains, California and Nevada. *Geol. Soc. Am. Bull*. **2003**, *115* (7), 788–816.
23. Ali, G.A.H.; Reiners, P.W.; Ducea, M.N. Unroofing history of Alabama and Poverty Hills basement blocks, Owens Valley, California, from apatite (U-Th)/He thermochronology. *Int. Geol. Rev*. **2009**, *51* (9/11), 1034–1050.
24. Lee, J.; Stockli, D.F.; Owen, L.A.; Finkel, R.C.; Kislitsyn, R. Exhumation of the Inyo Mountains, California: Implications for the timing of extension along the western boundary of the Basin and Range Province and distribution of dextral fault slip rates across the eastern California shear zone. *Tectonics* **2009**, *28*, TC1001:1–TC1001:20.
25. Monastero, F.C.; Walker, J.D.; Katzenstein, A.M.; Sabin, A.E. Neogene evolution of the Indian Wells Valley, east-central California. In *Geologic Evolution of the Mojave Desert and Southwestern Basin and Range*; Geological Society of America: Boulder Memoir 195; Glazner, A.F., Walker, J.D., Bartley, J.M., Eds.; Geological Society of America: Boulder, CO, USA, 2009; pp. 199–228.

26. Monastero, F.C.; Katzenstein, A.M.; Miller, J.S.; Unruh, J.R.; Adams, M.C.; Richards-Dinger, K. The Coso geothermal field: A nascent metamorphic core complex. *Geol. Soc. Am. Bull*. **2005**, *117* (11/12), 1534–1553.
27. Hollett, K.J.; Danskin, W.R.; McCaffrey, W.F.; Walti, C.L. *Geology and Water Resources of Owens Valley*, *California:* U.S. Geological Survey Water-Supply Paper 2370-B; U.S. Government Printing Office: Washington, DC, USA, 1991.
28. Phillips, F.M. Geological and hydrological history of the paleo-Owens River drainage since the late Miocene. In *Late Cenozoic Drainage History of the Southwestern Great Basin and Lower Colorado River Region: Geologic and Biotic Perspectives*; Geological Society of America Special Paper 439; Reheis, M.C., Hershler, R., Miller, D.M., Eds.; Geological Society of America: Boulder, CO, USA, 2008; pp. 115–150.
29. Umhoefer, P.J. Why did the southern Gulf of California rupture so rapidly?—Oblique divergence across hot, weak lithosphere along a tectonically active margin. *GSA Today* **2011**, *21*, 4–10.
30. Fletcher, J. Keynote: The opening of the Gulf of California: Temporal *vs.* spatial variations in rift kinematics. In Proceedings of 108th Annual Meeting of CAMWS (The Classical Association of the Middle West and South), Abstracts with Programs, Baton Rouge, LA, USA, 28–31 March 2012; Geological Society of America: Boulder, CO, USA, 2012; Volume 44, No. 3-1, p. 5.
31. Wernicke, B. Cenozoic extensional tectonics of the U.S. Cordillera. In *The Cordilleran Orogen: Conterminous U.S.*; The Geology of North America, Volume G-3*;* Burchfiel, B.C., Lipman, P.W., Zoback, M.L., Eds.; Geological Society of America: Boulder, CO, USA, 1992; pp. 553–581.
32. Jones, C.H.; Farmer, G.L.; Unruh, J. Tectonics of Pliocene removal of lithosphere of the Sierra Nevada, California. *Geol. Soc. Am. Bull*. **2004**, *116* (11/12), 1408–1422.
33. Le Pourhiet, L.; Gurnis, M.; Saleeby, J. Mantle instability beneath the Sierra Nevada mountains in California and Death Valley extension. *Earth Planet. Sci. Lett.* **2006**, *251*, 104–119.
34. Stevens, C.H.; Stone, P.; Dunne, G.C.; Greene, D.C.; Walker, J.D.; Swanson, B.J. Paleozoic and Mesozoic evolution of east-central California. *Int. Geol. Rev*. **1997**, *39*, 788–829.
35. Sullivan, W.A.; Law, R.D. Deformation path partitioning within the transpressional White Mountain shear zone, California and Nevada. *J. Struct. Geol.* **2006**, *29*, 583–598.
36. Conrad, J.E. Late Cenozoic Tectonics of the Southern Inyo Mountains, Eastern California. Master's Thesis, San Jose State University, San Jose, CA, USA, May 1993.
37. Amos, C.B.; Kelson, K.I.; Rood, D.H.; Simpson, D.T.; Rose, R.S. Late Quaternary slip rate on the Kern Canyon fault at Soda Spring, Tulare County, California. *Lithosphere* **2010**, *2* (6), 411–417.
38. Nadin, E.S.; Saleeby, J.B. Quaternary reactivation of the Kern Canyon fault system, southern Sierra Nevada, California. *Geol. Soc. Am. Bull*. **2010**, *122* (9/10), 1671–1685.
39. Brossy, C.C.; Kelson, K.I.; Amos, C.B.; Baldwin, J.N.; Kozlowicz, B.; Simpson, D.; Ticci, M.G.; Lutz, A.T.; Kozaci, O.; Streig, A.; *et al.* Map of the late Quaternary active Kern Canyon and Breckenridge faults, southern Sierra Nevada, California. *Geosphere* **2012**, *8* (3), 581–591.
40. Pakiser, L.C.; Kane, M.F.; Jackson, W.H. *Structural Geology and Volcanism of Owens Valley Region*, *California—A Geophysical Study*; U.S. Geological Survey Professional Paper 438; U.S. Government Printing Office: Washington, DC, USA, 1964.
41. Dixon, T.H.; Robaudo, S.; Lee, J.; Reheis, M.C. Constraints on the present day Basin and Range deformation from space geodesy. *Tectonics* **1995**, *14* (4), 755–772.

42. Lee, J.; Le, K. Active faulting in Owens Valley, California. In *Western Great Basin Geology, Fieldtrip Guidebook and Volume*; Pacific Section SEPM Book 99; Stevens, C.H., Cooper, J., Eds.; Pacific Section SEPM: Santa Fe Springs, CA, USA, 2005; pp. 3–10.
43. Le, K.; Lee, J.; Owen, L.A.; Finkel, R. Late Quaternary slip rates along the Sierra Nevada frontal fault zone, California: Slip partitioning across the western margin of the Eastern California Shear Zone-Basin and Range Province. *Geol. Soc. Am. Bull*. **2007**, *119* (1/2), 240–256.
44. Roquemore, G. Structure, tectonics, and stress field of the Coso Range, Inyo County, California. *J. Geophys. Res*. **1980**, *85* (B5), 2434–2440.
45. Amos, C.B. Geology Department, Western Washington University. Personal Communication, 2013.
46. Unruh, J.R.; Hauksson, E.; Monastero, F.C.; Twiss, R.J.; Lewis, J.C. Seismotectonics of the Coso Range-Indian Wells Valley region, California: Transtensional deformation along the southeastern margin of the Sierran microplate. In *Geologic Evolution of the Mojave Desert and Southwestern Basin and Range*; Geological Society of America Memoir 195; Glazner, A.F., Walker, J.D., Bartley, J.M., Eds.; Geological Society of America: Boulder, CO, USA, 2009; pp. 277–294.
47. Reheis, M.C.; Dixon, T.H. Kinematics of the eastern California shear zone: Evidence for slip transfer from Owens and Saline Valley fault zones to Fish Lake Valley fault zone. *Geology* **1996**, *24* (4), 339–342.
48. Lee, J.; Rubin, C.M.; Calvert, A. Quaternary faulting history along the Deep Springs fault, California. *Geol. Soc. Am. Bull.* **2001**, *113* (7), 855–869.
49. Bishop, K.M.; Clements, S. The Poverty Hills, Owens Valley, California—Transpressional uplift or ancient landslide deposit? *Env. Eng. Geosci*. **2006**, *12* (4), 301–314.
50. U.S. Geological Survey Web Page. Quaternary Fault and Fold Database of the United States. Available online: http://earthquake.usgs.gov/hazards/qfaults/ (accessed on 27 March 2012).
51. Lewis, J.C.; Twiss, R.J.; Pluhar, C.J.; Monastero, F.C. Multiple constraints on divergent strike-slip deformation along the eastern margin of the Sierran microplate, SE California. In *Exhumation Associated with Continental Strike-Slip Fault Systems*; Geological Society of America Special Paper 434; Till, A.B., Roeske, S.M., Foster, D.A., Sample, J.C., Eds.; Geological Society of America: Boulder, CO, USA, 2007; pp. 107–128.
52. Blakely, R.J. *Potential Theory in Gravity and Magnetic Applications*; Cambridge University Press: New York, NY, USA, 1995.
53. Simpson, R.W.; Jachens, R.C.; Blakely, R.J.; Saltus, R.W. A new isostatic residual gravity map of the conterminous United States with a discussion of the significance of isostatic residual anomalies. *J. Geophy. Res.* **1986**, *91* (B8), 8348–8372.
54. Bateman, P.C.; Pakiser, L.C.; Kane, M.F. *Geology and Tungsten Mineralization of the Bishop District*, *California*, *with a Section on Gravity Study of Owens Valley and a Section on Seismic Profile*; U.S. Geological Survey Professional Paper 470; U.S. Government Printing Office: Washington, DC, USA, 1965.
55. Blakely, R.J.; Jachens, R.C.; Calzia, J.P.; Langenheim, V.E. Cenozoic basins of the Death Valley extended terrane as reflected in regional-scale gravity anomalies. In *Cenozoic Basins of the Death Valley Region*; Geological Society of America Special Paper 333; Wright, L.A., Troxel, B.W., Eds.; Geological Society of America: Boulder, CO, USA, 1999; pp. 1–16.

56. Saltus, R.W.; Jachens, R.C. *Gravity and Basin Depth Maps for the Basin and Range Province*, *Western United States*; U.S. Geological Survey Geophysical Map GP-1012; U.S. Government Printing Office: Washington, DC, USA, 1995; Scale 1:250,000.
57. Jachens, R.C.; Moring, B.C. *Maps of Thickness of Cenozoic Deposits and the Isostatic Residual Gravity over Basement for Nevada*; U.S. Geological Survey Open-File Report 90-404; U.S. Government Printing Office: Washington, DC, USA, 1990; Scale 1:1,000,000.
58. Pluhar, C.J.; Coe, R.S.; Lewis, J.C.; Monastero, F.C.; Glen, J.M.G. Fault block kinematics at a releasing stepover of the Eastern California shear zone: Partitioning of rotation style in and around the Coso geothermal area and nascent metamorphic core complex. *Earth Planet. Sci. Lett.* **2006**, *250*, 134–163.
59. University of California, Berkeley, Seismological Laboratory Seismo Blog Web Page. Triple Shock in Owens Valley. Available online: http://seismo.berkeley.edu/blog/seismoblog.php/2009/10/05/triple-shock-in-owens-valley (accessed on 2 November 2012).
60. Hoylman, E.W. The Geology of the Poverty Hills area, Inyo County, California. Master's Thesis, University of California, Los Angeles, CA, USA, 1974.
61. Stevens, C.H.; Greene, D.C. Stratigraphy, depositional history, and tectonic evolution of Paleozoic continental-margin rocks in roof pendants of the eastern Sierra Nevada, California. *Geol. Soc. Am. Bull.* **1999**, *111* (6), 919–933.
62. Martel, S.J. Structure and late Quaternary activity of the northern Owens Valley fault zone, Owens Valley, California. *Eng. Geol*. **1989**, *27*, 489–507.
63. Taylor, T.R. Origin and Structure of the Poverty Hills, Owens Valley Fault Zone, Owens Valley, California. Master's Thesis, Miami University, Oxford, OH, USA, 2002.
64. Stevens, C.H.; Stone, P.; Bishop, K.M.; Blakely, R.J. A new hypothesis for the origin of the Poverty Hills, Owens Valley, California. In Proceedings of 106th Annual Meeting, and Pacific Section, American Association of Petroleum Geologists, Abstracts with Programs, Anaheim, CA, USA, 27–29 May 2010; Geological Society of America: Boulder, CO, USA, 2010; Volume 42, No. 12-3, p. 55.
65. Bailey, R.A. Geologic Map of Long Valley Caldera, Mono-Inyo Craters Volcanic Chain *and Vicinity*, *Eastern California*; U.S. Geological Survey Miscellaneous Investigations Map I-1933; U.S. Government Printing Office: Washington, DC, USA, 2010.
66. Nadin, E.S.; Saleeby, J.B. Disruption of regional primary structure of the Sierra Nevada batholiths by the Kern Canyon fault system, California. In *Ophiolites, Arcs, and Batholiths: A Tribute to Cliff Hopson*; Geological Society of America Special Paper 438; Wright, J.E., Shervais, J.W., Eds.; Geological Society of America: Boulder, CO, USA, 2008; pp. 429–454.
67. Maheo, G.; Saleeby, J.; Saleeby, Z.; Farley, K.A. Tectonic control on southern Sierra Nevada topography, California. *Tectonics* **2009**, *28*, TC6006:1–TC6006:22.
68. Wesnousky, S.G.; Jones, C.H. Oblique slip, slip partitioning, spatial and temporal changes in the regional stress field, and the relative strength of active faults in the Basin and Range, western United States. *Geology* **1994**, *22* (11), 1031–1034.

69. Stone, P.; Dunne, G.C.; Stevens, C.H.; Gulliver, R.M. *Geologic Map of Paleozoic and Mesozoic Rocks in Parts of the Darwin and Adjacent Quadrangles, Inyo County, California*; U.S. Geological Survey Miscellaneous Investigation Series Map I-1932; U.S. Government Printing Office: Washington, DC, USA, 1989; Scale 1:31,250.
70. Schweig, E.S., III. Basin-range tectonics in the Darwin Plateau, southwestern Great Basin, California. *Geol. Soc. Am. Bull.* **1989**, *101* (5), 652–662.
71. Nelson, C.A. *Geologic Map of the Waucoba Mountain Quadrangle, Inyo County, California*; U.S. Geological Survey Geologic Quadrangle Map GQ-528; U.S. Government Printing Office: Washington, DC, USA, 1966; Scale 1:62,500.
72. Streitz, R.; Stinson, M.C. *Geologic Map of California, Death Valley Sheet*; California Division of Mines and Geology: Sacramento, CA, USA, 1977; Scale 1:250,000.
73. Strand, R.G. *Geologic Map of California, Mariposa Sheet*; California Division of Mines and Geology: Sacramento, CA, USA, 1967; Scale 1:250,000.
74. Amos, C.B.; Fisher, G.B., III; Rood, D.H.; Jayko, A.S.; Burgmann, R. New Terrestrial, LIDAR and Cosmogenic Radionuclide Constraints on the Little Lake Fault, Eastern California Shear Zone; Annual Reports; Berkeley Seismological Laboratory: Berkeley, CA, USA, 2007. Available online: http://seismo.berkeley.edu/annual_report/ar09_10/node5.html (accessed on 12 April 2013).
75. Loomis, D.P.; Burbank, D.W. The stratigraphic evolution of the El Paso basin, southern California: Implications for the Miocene development of the Garlock fault and uplift of the Sierra Nevada. *Geol. Soc. Am. Bull.* **1988**, *100* (1), 12–28.
76. Andrew, J.E.; Walker, J.D.; Monastero, F.C. Initiation and slip history of the central segment of the Garlock Fault, California. In Proceedings of 2011 GSA (Geological Society of America) Annual Meeting in Minneapolis, Minneapolis, MN, USA, 9–12 October 2011; Geological Society of America: Boulder, CO, USA, 2011; Volume 43, No. 55, p. 35.
77. Rinehart, C.D.; Ross, D.C. *Geology of the Casa Diablo Mountain Quadrangle*, *California*; U.S. Geological Survey Geologic Quadrangle Map GQ 99; U.S. Government Printing Office: Washington, DC, USA, 1957; Scale 1:62,500.
78. Jennings, C.W.; Burnett, J.L.; Troxel, B.W. *Geologic Map of California, Trona Sheet*; California Division of Mines and Geology: Sacramento, CA, USA, 1962; Scale 1:250,000.
79. Matthews, R.A.; Burnett, J.L. *Geologic Map of California, Fresno Sheet*; California Division of Mines and Geology: Sacramento, CA, USA, 1965; Scale 1:250,000.
80. Crowder, D.F.; Sheridan, M.F. *Geologic Map of the White Mountain Peak Quadrangle, Mono County, California*; U.S. Geological Survey Map GQ-1012; U.S. Government Printing Office: Washington, DC, USA, 1972; Scale 1:62,500.
81. Walker, J.D.; Berry, A.K.; Davis, P.J.; Andrew, J.E.; Mitsdarfer, J.M. Geologic map of northern Mojave Desert and southwestern Basin and Range, California. In *Geologic Evolution of the Mojave Desert and Southwestern Basin and Range*; Geological Society of America Memoir 195; Glazner, A.F., Walker, J.D., Bartley, J.M., Eds.; Geological Society of America: Boulder, CO, USA, 2009; Plate 1, Scale 1:250,000.
82. Stinson, M.C. *Geology of the Haiwee Reservoir 15' Quadrangle*, *Inyo County*, *California*; California Division of Mines and Geology Map Sheet 37; California Division of Mines and Geology: Sacramento, CA, USA, 1977; Scale 1:62,500.

83. Duffield, W.A.; Bacon, C.R.; Dalrymple, G.B. Late Cenozoic volcanism, geochronology, and structure of the Coso Range, Inyo County, California. *J. Geophys. Res*. **1980**, *85* (B5), 2381–2404.
84. Duffield, W.A.; Bacon, C.R. *Geologic Map of the Coso Volcanic Field and Adjacent Areas, Inyo County, California*; U.S. Geological Survey Miscellaneous Investigations Map I-1200; U.S. Government Printing Office: Washington, DC, USA, 1981; Scale 1:50,000.
85. Bacon, C.R.; Giovannetti, D.M.; Duffield, W.A.; Dalrymple, G.B.; Drake, R.E. *Age of the Coso Formation, Inyo County, California*; U.S. Geological Survey Bulletin 1527; U.S. Government Printing Office: Washington, DC, USA, 1982.
86. Jayko, A.S. *Surficial Geologic Map of the Darwin Hills 30′ × 60′ Quadrangle, Inyo County, California*; U.S. Geological Survey Scientific Investigations Map 3040; U.S. Government Printing Office: Washington, DC, USA, 2009; Scale 1:100,000.
87. Hall, W.E.; MacKevett, E.M., Jr. *Geology and Ore Deposits of the Darwin Quadrangle, Inyo County, California*; U.S. Geological Survey Professional Paper 368; U.S. Government Printing Office: Washington, DC, USA, 1962.
88. Duffield, W.A.; Roquemore, G.R. Late Cenozoic volcanism and tectonism in the Coso Range area, California. In *This Extended Land: Geological Journeys in the Southern Basin and Range*; UNLV Department of Geosciences Special Pubication 2; Weide, D.L., Faber, M.L., Eds.; University of Nevada: Las Vegas, NV, USA, 1988; pp. 159–175.
89. Stinson, M.C. *Geology of the Keeler 15' Quadrangle, Inyo County*, *California*; California Division of Mines and Geology Map Sheet 38; California Division of Mines and Geology: Sacramento, CA, USA, 1977; Scale 1:62,500.
90. Faulds, J.E.; Varga, R.J. The role of accommodation zones and transfer zones in the regional segmentation of extended terranes. In *Accommodation Zones and Transfer Zones: The regional Segmentation of the Basin and Range Province*; Geological Society of America Special Paper 323; Faulds, J.E., Stewart, J.H., Eds.; Geological Society of America: Boulder, CO, USA, 1998; pp. 1–45.
91. Bacon, S.N.; Jayko, A.S.; McGeehin, J.P. Holocene and latest Pleistocene oblique dextral faulting on the Southern Inyo Mountains Fault, Owens Lake basin, California. *Bull. Seismol. Soc. Am.* **2005**, *95* (6), 2472–2485.
92. Stone, P.; Swanson, B.J.; Stevens, C.H.; Dunne, G.C.; Priest, S.S. *Geologic Map of the Southern Inyo Mountains and Vicinity, Inyo County, California*; U.S. Geological Survey Scientific Investigations Map 3094; U.S. Geological Survey: Menlo Park, CA, USA, 2009; Scale 1:24,000. Available online: http://pubs.usgs.gov/sim/3094 (accessed on 12 April 2013).
93. Smith, G.I. Stratigraphy, lithologies, and sedimentary structures of Owens Lake core OL-92. In *An 800,000-Year Paleoclimatic Record from Core OL-92*, *Owens Lake*, *Southeast California*; Geological Society of America Special Paper 317; Smith, G.I., Bischoff, J.L., Eds.; Geological Society of America: Boulder, CO, USA, 1997; pp. 9–22.
94. Stone, P.; Dunne, G.C.; Conrad, J.E.; Swanson, B.J.; Stevens, C.H.; Valin, Z.C. *Geologic Map of the Cerro Gordo Peak 7.5' Quadrangle*, *Inyo County*, *California*; US Geological Survey Scientific Investigations Map 2851; U.S. Geological Survey: Menlo Park, CA, USA, 2004; Scale 1:24,000. Available online: http://pubs.usgs.gov/sim/2004/2851/ (accessed on 12 April 2013).

95. Ross, D.C. *Geology of the Independence Quadrangle*, *Inyo County*, *California*; U.S. Geological Survey Bulletin 1181-O; U.S. Government Printing Office: Washington, DC, USA, 1965.
96. Berman, F.A. The paleoclimate and tectonic significance of the Bee Springs alluvial fan sequence, west-central Inyo Mountains, east central California. Master's Thesis, Humboldt State University, Arcata, CA, USA, 1999.
97. Maheo, G.; Farley, K.A.; Clark, M.K. Cooling and exhumation of the Sierra Nevada batholith in the Mount Whitney area (California) based on (U-Th)/He thermochronometry. *Eos* **2004**, *85* (47), F1745.
98. Lueddecke, S.B.; Pinter, N.; Gans, P. Plio-Pleistocene ash falls, sedimentation, and range-front faulting along the White-Inyo Mountains front, California. *J. Geol*. **1998**, *106*, 511–522.
99. Bachman, S.B. Pliocene-Pleistocene break-up of the Sierra Nevada–White-Inyo Mountains block and formation of Owens Valley. *Geology* **1978**, *6*, 461–463.
100. Sarna-Wojcicki, A.M.; Reheis, M.C.; Pringle, M.S.; Fleck, R.J.; Burbank, D.; Meyer, C.E.; Slate, J.L.; Wan, E.; Budahn, J.R.; Troxel, B.; Walker, J.P. *Tephra Layers of Blind Spring Valley and Related Upper Pliocene and Pleistocene Tephra Layers, California, Nevada, and Utah: Isotopic Ages, Correlation, and Magnetostratigraphy*; U.S. Geological Survey Professional Paper 1701; U.S. Government Printing Office: Washington, DC, USA, 2005.
101. Phillips, F.M.; McIntosh, W.C.; Dunbar, N.N. The chronology of late Cenozoic volcanic eruptions onto relict surfaces in the south-central Sierra Nevada, California. *Geol. Soc. Am. Bull*. **2011**, *123* (5/6), 890–910.
102. Chen, J.H.; Moore, J.G. Uranium-lead isotopic ages from the Sierra Nevada batholith, California. *J. Geophys. Res*. **1982**, *87* (B6), 4761–4784.
103. House, M.A.; Wernicke, B.P.; Farley, K.A. Paleo-geomorphology of the Sierra Nevada, California, from (U-Th)/He ages in apatite. *Am. J. Sci*. **2001**, *301*, 77–102.
104. Clark, M.K.; Maheo, G.; Saleeby, J.; Farley, K.A. The non-equilibrium landscape of the southern Sierra Nevada, California. *GSA Today* **2005**, *15* (9), 4–10.
105. Stevens, C.H.; Stone, P. Correlation of Permian and Triassic deformations in the western Great Basin and eastern Sierra Nevada: Evidence from the northern Inyo Mountains near Tinemaha Reservoir, east-central California. *Geol. Soc. Am. Bull*. **2002**, *114* (10), 1210–1221.
106. Bartley, J.M.; Glazner, A.F.; Coleman, D.S.; Kylander-Clark, A.; Greene, D.C. Bedrock evidence for 65 km of dextral offset. In *Western Great Basin Geology, Fieldtrip Guidebook and Volume*; Pacific Section SEPM Book 99; Stevens, C.H., Cooper, J., Eds.; Pacific Section SEPM: Santa Fe Springs, CA, USA, 2005; pp. 11–16.
107. Renne, P.R.; Turrin, B.D. Constraints on timing of deformation in the Benton Range, southeastern California, and implications of Nevadan orogenesis. *Geology* **1987**, *15*, 1031–1034.
108. Wood, D.J.; Saleeby, J.B. Late Cretaceous-Paleocene extensional collapse and disaggregation of the southernmost Sierra Nevada batholiths. *Int. Geol. Rev.* **1997**, *39*, 973–1009.
109. Chapman, A.D.; Saleeby, J.B.; Wood, D.J.; Piasecki, A.; Kidder, S.; Ducea, M.N.; Farley, K.A. Late Cretaceous gravitational collapse of the southern Sierra Nevada batholith, California. *Geosphere* **2012**, *8* (2), 314–341.

110. Engebretson, D.C.; Cox, A.; Gordon, R.G. *Relative Motions between Oceanic and Continental Plates in the Pacific Basin*; Geological Society of America Special Paper 206; Geological Society of America: Boulder, CO, USA, 1985.
111. Kanter, L.R.; McWilliams, M.O. Rotation of the southernmost Sierra Nevada, California. *J. Geophys. Res.* **1982**, *87* (B5), 3819–3830.
112. Dunne, G.C.; Suzcek, C.A. Early Paleozoic eugeoclinal strata in the Kern Plateau pendants, southern Sierra Nevada, California. In *Paleozoic Paleogeography of the Western United States-II*; Pacific Section SEPM Book 67; Cooper, J.D., Stevens, C.H., Eds.; Pacific Section SEPM: Bakersfield, CA, USA; Volume 2, pp. 677–692.
113. McPhillips, D.; Brandon, M.T. Topographic evolution of the Sierra Nevada measured directly by inversion of low-temperature thermochronology. *Am. J. Sci*. **2012**, *312*, 90–116.
114. Andrew, J.E.; Walker, J.D. Reconstructing late Cenozoic deformation in central Panamint Valley, California: Evolution of slip partitioning in the Walker Lane. *Geosphere* **2009**, *5* (3), 172–198.
115. Hodges, K.V.; McKenna, L.W.; Harding, M.B. Structural unroofing of the central Panamint Mountains, Death Valley region, southeastern California. In *Basin and Range Extensional Tectonics near the Latitude of Las Vegas, Nevad*a; Wernicke, B.P., Ed.; Geological Society of America Memoir 176; Geological Society of America: Boulder, CO, USA, 1990; pp. 377–390.
116. Blakely, R.J.; McKee, E.H. Subsurface structural features of the Saline Range and adjacent regions of eastern California as interpreted from isostatic residual gravity anomalies. *Geology* **1985**, *13* (1), 781–785.
117. Burchfiel, B.C.; Hodges, K.V.; Royden, L.H. Geology of Panamint Valley-Saline Valley pull-apart system, California: Palinspastic evidence for low-angle geometry of a Neogene range-bounding fault. *J. Geophys. Res.* **1987**, *92* (B10), 10422–10426.
118. MIT 1985 Field Geophysics Course; Biehler, S. A geophysical investigation of the northern Panamint Valley, Inyo County, California: Evidence for possible low-angle normal faulting at shallow depth in the crust. *J. Geophys. Res*. **1987**, *92* (B10), 10427–10441.
119. Hamilton, W.B. Detachment faulting in the Death Valley region, California and Nevada. In *Geologic and Hydrologic Investigations of a Potential Nuclear Waste Disposal Site at Yucca Mountain, Southern Nevada*; U.S. Geological Survey Bulletin 1790; Carr, M.C., Yount, J.C., Eds.; U.S. Government Printing Office: Washington, DC, USA, 1988; pp. 51–85.
120. Cichanski, M. Low-angle, range-flank faults in the Panamint, Inyo, and Slate ranges, California: Implications for recent tectonics of the Death Valley region. *Geol. Soc. Am. Bull*. **2000**, *112* (6), 871–883.
121. Numelin, T.; Marone, C.; Kirby, E. Frictional properties of natural fault gouge from a low-angle normal fault, Panamint Valley, California. *Tectonics* **2007**, *26*, TC2004:1–TC2004:14.
122. Norton, I. Two-stage formation of Death Valley. *Geosphere* **2011**, *7* (1), 171–182.
123. Ducea, M.; Saleeby, J. A case for delamination of the deep batholithic crust beneath the Sierra Nevada, California. *Int. Geol. Rev*. **1998**, *40*, 78–93.
124. Poage, M.A.; Chamberlain, C.P. Empirical relationships between elevation and the stable isotope composition of precipitation and surface waters: Considerations for studies of paleoelevation change. *Am. J. Sci*. **2001**, *301*, 1–15.

125. Horton, T.W.; Chamberlain, C.P. Stable isotopic evidence for Neogene surface downdrop in the central Basin and Range Province. *Geol. Soc. Am. Bull.* **2006**, *118* (3/4), 475–490.
126. Molnar, P. Deuterium and oxygen isotopes, paleoelevations of the Sierra Nevada, and Cenozoic climate. *Geol. Soc. Am. Bull.* **2010**, *122* (7/8), 1106–1115.
127. Ferrari, L.; Orozco-Esquival, T.; Lopez Martinez, M.; Duque, J.; Bryan, S.; Cerca, M. 25 million years to break a continent: Early to middle Miocene rifting and syn-extensional magmatism in the southern Gulf of California. In Proceedings of 108th Annual Meeting of CAMWS (The Classical Association of the Middle West and South), Abstracts with Programs, Baton Rouge, LA, USA, 28–31 March 2012; Geological Society of America: Boulder, CO, USA, 2012; Volume 44, No. 3-7, p. 6.
128. Bennett, S.E.K.; Oskin, M.E.; Iriondo, A. Progressive localization of dextral shear in the late Proto-Gulf of California. In Proceedings of 108th Annual Meeting of CAMWS (The Classical Association of the Middle West and South), Abstracts with Programs, Baton Rouge, LA, USA, 28–31 March 2012; Geological Society of America: Boulder, CO, USA, 2012; Volume 44, No. 3-4, p. 5.
129. Martin, A.; Gonzalez-Escobar, M.; Fletcher, J.; Pacheco, M. Continental rupture delayed by sedimentation and low-angle normal faults in the northern Gulf of California: Analysis of seismic reflection profiles in the Tiburon and Delfin basins. In Proceedings of 108th Annual Meeting of CAMWS (The Classical Association of the Middle West and South), Abstracts with Programs, Baton Rouge, LA, USA, 28–31 March 2012; Geological Society of America: Boulder, CO, USA, 2012; Volume 44, No. 3-2, p. 5.
130. McClusky, S.C.; Bjornstad, S.C.; Hager, B.H.; King, R.W.; Meade, B.J.; Miller, M.M.; Monastero, F.C.; Souter, B.J. Present day kinematics of the Eastern California Shear Zone from a geodetically constrained block model. *Geophys. Res. Lett.* **2001**, *28* (17), 3369–3372.
131. Frankel, K.L.; Glazner, A.F.; Kirby, E.; Monastero, F.C.; Strane, M.D.; Oskin, M.E.; Unruh, J.R.; Walker, J.D.; Anandakrishnan, S.; Bartley, J.M.; *et al.* Active tectonics of the eastern California shear zone. In *Field Guide to Plutons, Volcanoes, Faults, Reefs, Dinosaurs, and Possible Glaciations in Selected Areas of Arizona, California, and Nevada*; Geological Society of America Field Guide 11; Duebendorfer, E.M., Smith, E.I., Eds.; Geological Society of America: Boulder, CO, USA, 2008; pp. 43–81.